ANALYSIS OF HEART RATE VARIABILITY DURING FOCAL PARASYMPATHETIC DRIVE OF THE RAT BAROREFLEX

A Thesis

Submitted to the Faculty

of

Purdue University

by

David J. Bustamante

In Partial Fulfillment of the

Requirements for the Degree

of

Masters of Science in Biomedical Engineering

May 2020

Purdue University

Indianapolis, Indiana

THE PURDUE UNIVERSITY GRADUATE SCHOOL
STATEMENT OF THESIS APPROVAL

Dr. John Schild, Chair

Department of Biomedical Engineering

Dr. Ken Yoshida

Department of Biomedical Engineering

Dr. Paul Salama

Department of Electrical and Computer Engineering

Approved by:

Dr. Julie Ji

Head of the Graduate Program

ACKNOWLEDGMENTS

Sidnee Zeiser for her assistance in many of the surgical protocols carried out in this thesis.

TABLE OF CONTENTS

Page

Page

LIST OF TABLES

LIST OF FIGURES

Figure Page

Figure Page

ABSTRACT

Bustamante, David J M.S.B.M.E., Purdue University, May 2020. Analysis of Heart Rate Variability During Focal Parasympathetic Drive of the Rat Baroreflex. Major Professor: John Schild.

Autonomic control of the heart results in variations in the intervals between heart beats, known as heart rate variability. One of the defining components of autonomic control is the baroreflex, a negative feedback controller that balances heart rate and blood pressure. The baroreflex is under constant command from the branches of the autonomic nervous system. To better understand how the autonomic nervous system commands the baroreflex, a baroreflex reflexogenic animal protocol was carried out. Heart rate variability analysis and baroreflex sensitivity were used to quantify the neural control of the heart. This thesis reconfirmed the existence of sexually dimorphic properties in the baroreflex through the use of heart rate variability analysis and baroreflex sensitivity. It was discovered that there are many caveats to utilizing heart rate variability analysis, which have to be addressed both in the experimental protocol and the signal processing technique. Furthermore, it was suggested that the slope method for quantifying baroreflex sensitivity also has many caveats, and that other baroreflex sensitivity methods are likely more optimal for quantifying sustained activation of the baroreflex. By utilizing various heart rate variability signal processing algorithms to assess autonomic tone in Sprague-Dawley rats during rest and sustained electrical activation of the baroreflex, the null hypothesis was rejected.

CHAPTER 1. INTRODUCTION

1.1 Quantitative Assessment of Autonomic Tone in Cardiovascular Homeostasis

1.1.1 Background and Historical Significance

Since 1921, cardiovascular disease (CVD) has been the leading cause of death in the United States [1]. In 2017, CVD was cited as the cause of death of about 650,000 people in the US, and about 18,000,000 worldwide [2]. Since 1950, CVD has decreased by about 60 percent in the United States, but still accounts for a fourth of all annual deaths in the US, surpassing cancer and all other diseases. The decrease has been largely the result of advances in clinical understanding of cardiovascular health and disease along with advances in technology, clinical intervention techniques, pharmaceuticals, and lifestyle changes that promote a more healthy cardiovascular physiology [1]. Nonetheless, the worldwide prevalence of CVD continues to increase. The most common risk factors include an unhealthy diet, lack of physical activity, consumption of alcohol, and tobacco use [1]. Several risks are hereditary. The CDC reports CVD prevalence is higher in men than women [1]. Whites and African Americans have the highest prevalence of CVD in the US [1]. Prevalence of CVD in people above 50 years old is more than an order of magnitude higher than those below 25 [1].

Two of the most commonly utilized methods for assessing cardiovascular health are measures of blood pressure (BP) and heart rate (HR). These measurements are taken in clinics because they are procedurally simple, inexpensive, and noninvasive.

They have high correlation to the overall function of the cardiovascular system (CVS) and a high BP or abnormal HR are two of the highest risk factors for CVD [2, 3].

There is an on-going demand for easily implementable and non-invasive diagnostic measures like BP and HR in modern medicine. In the last fifty years, more methodologies have evolved, often involving sophisticated signal processing techniques. These utilize complex algorithms to extract useful information about the health of a patient while remaining non-invasive and simple to implement, making them useful in clinical practice. These methodologies rely on the data collected from common clinical tests such as drug infusion (e.g. nitroglycerin or phenylephrine) or mechanical tests (e.g. tilt table or treadmill).

1.1.2 Anatomy, Physiology, and Neural Control of the Heart

The heart is a muscular organ that drives blood flow by contracting to push the blood through its four chambers, termed the atria and ventricles (figure 1.1). This is a repetitive cycle that allows the blood to be oxygenated in the lungs, distributed to peripheral and central arterial circulation, and returned to the right atrium via the venous network where the deoxygenated blood is returned to the lungs [4]. The timing and intensity of the contractions of the heart are under both neuronal and hormonal control. These control pathways work together to ensure that cardiac output meets physiological demand.

The body is constantly driven to maintain a sufficient level of cardiac output, an effort known as cardiovascular homeostasis. This effort largely manifests as blood being transported and directed per the metabolic and hemodynamic demands needed by each organ system. This balance is maintained by neural and hormonal mechanisms that are predominately associated with the autonomic nervous system (ANS) acting by sympathetic and parasympathetic pathways. This is accomplished through the action of a highly integrated network of sensory feedback pathways and central neural circuitry of the ANS.

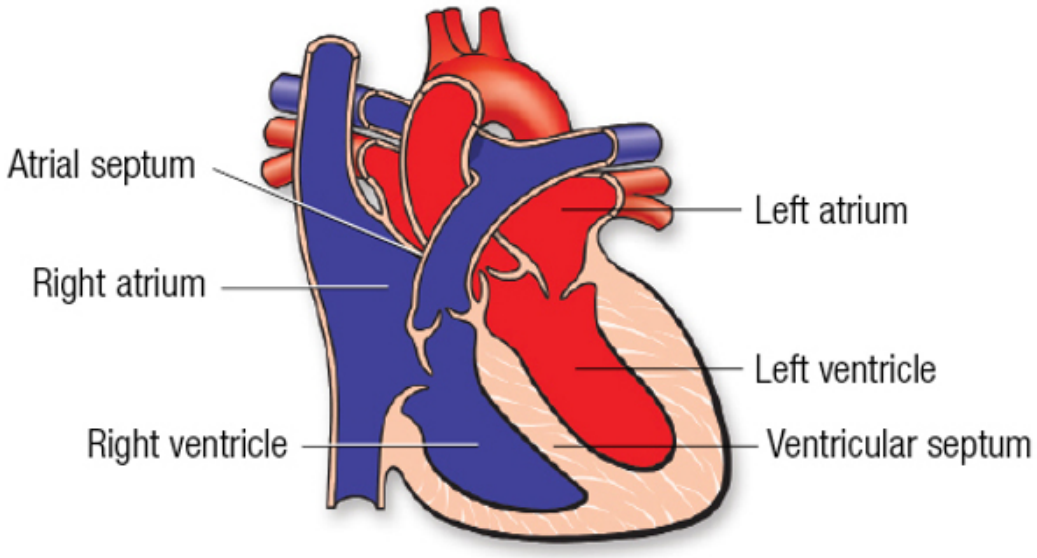

Fig. 1.1 Diagram of the heart [4]. Deoxygenated blood (blue) travels through the right side of the heart before being reoxygenated (red) in the lungs. It then travels through the left side of the heart and into the rest of the body.

1.1.3 Rhythmic Control of the Heart

There is an active coordination between respiration and HR that is termed respiratory sinus arrhythmia (RSA) [5–7]. During inspiration, HR increases while during expiration, HR decreases, resulting in a cyclical HR. This phenomenon is controlled by the brain primarily through the vagal nerve, with minimal sympathetic nervous system influence [5]. RSA is beneficial for perfusion of oxygen in the lungs and energy conservation [5,6]. By modulating the timing of the HR, it allows for a more efficient absorption of oxygen into the blood.

There is also a coordination between BP and HR termed the baroreceptor reflex (BRx). The BRx is mediated by stress-sensing nerve endings called baroreceptors. Baroreceptors are mechanical receptors that detect changes in BP and communicate those changes to the central nervous system (CNS) [8]. Any neural activity encoded in the peripherals and sent as an input to the CNS is termed afferent communication.

The CNS responds appropriately to BP changes by sending information to alter HR as necessary. This output to the peripherals is termed efferent communication.

All neural and hormonal control mechanisms such as RSA and the BRx each have a designated structure of afferent and efferent fibers, forming a sophisticated neuroanatomical structure. When one controller generates a perturbation, it has rippling effects. There is a ceaseless exchange of information, creating a constant oscillation around cardiovascular homeostasis.

1.1.4 Clinical Assessment of Cardiovascular Homeostasis

Electrocardiography is the study of the electrical propagation of activity in the heart. This is most often accomplished by measuring the faint voltage fields generated at the body surface from the electrical activity of the heart by using patch electrodes, termed a surface electrocardiogram (ECG). Such signals can provide critically important information about the electrical and mechanical state of the heart. The heart's electrical pathway is defined by spatial and temporal components that integrate to form the commonly seen P-QRS-T complex (figure 1.2).

An ECG provides information about the rate, rhythmicity, depolarization, conduction, and contraction of the heart. HR is often obtained by measuring the time series of the distinct R waves, which each indicate the contraction of the ventricles in the heart. Heart rhythm refers to the proper timing and coordination of the heartbeats in sequence. When heart rhythm is off, the beating can be slow, fast, or irregular. Depolarization (ion exchange) of the pacemaker cells in the heart create impulses to drive the sequential electrical pathway. Problems with depolarization can cause irregularities in the heart rhythm. Conduction is the ability of the heart cells to sequentially depolarize, allowing the formation of a continuous chronological pathway. Problems with conduction can severely hinder the heart's electrical function and thus are involved in most arrhythmias. Contraction is the result of the electrical

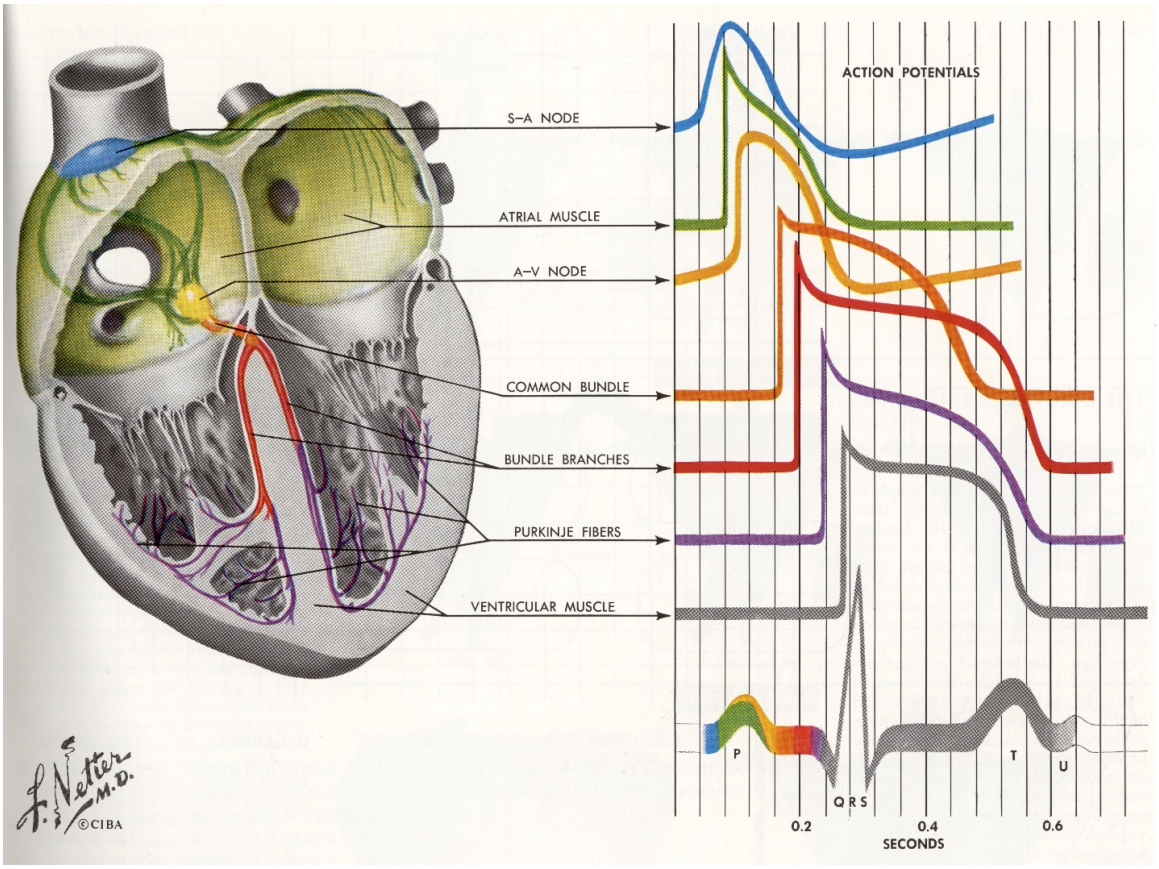

Fig. 1.2 Netter's diagram of human ECG [9]. The combined and sequential efforts of the electrophysiological anatomy create an overall ECG (seen at bottom right).

impulses driving muscle fibers in each chamber of the heart. The morphology of the ECG indicates if the heart is contracting properly and driving blood flow sufficiently.

Humans and rats have remarkably similar cardiovascular anatomy, although a rat's ECG (figure 1.3) has subtle differences in waveforms and a faster rate. Each waveform in the rat's ECG represents the same fundamental mechanical process as in the human heart. A rat's typical HR (5Hz) is about five times greater than a human's (1Hz), thus each waveform in the rat's ECG is significantly shorter than a corresponding human.

Like a human heart, a rat's heartbeat is not metronomic, but contains some small variability between each beat on the order of milliseconds (figure 1.3). This difference in successive periods of heartbeats is known as heart rate variability (HRV).

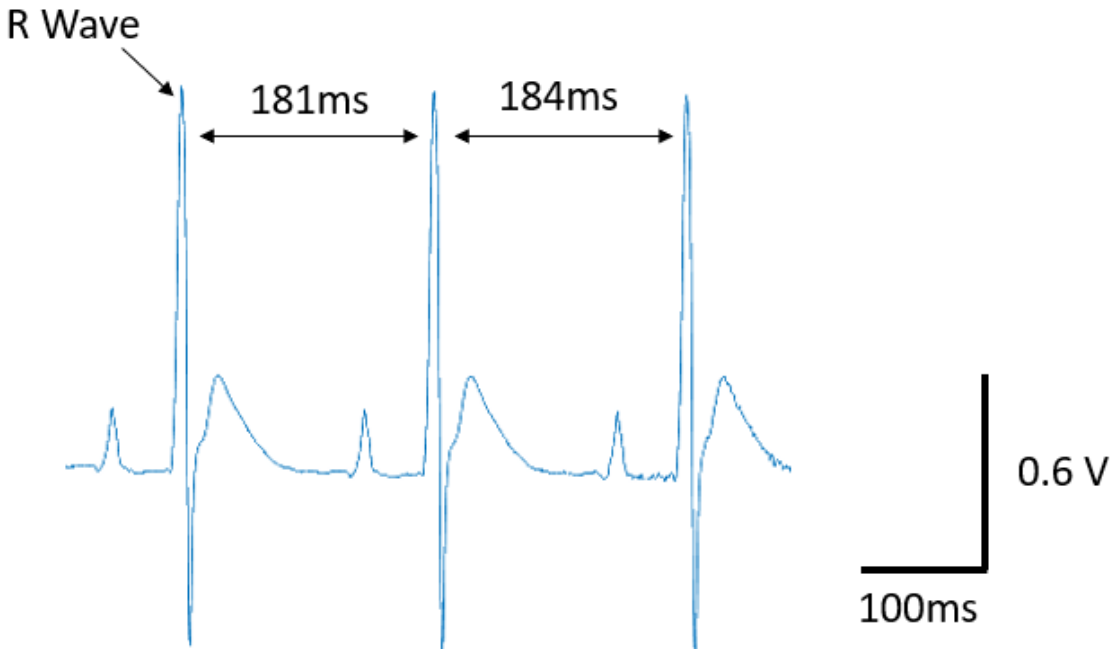

Fig. 1.3 Rat ECG

Blood pressure refers to the amount of pressure (in mmHg) the blood is exerting on the walls of the arteries. The American Heart Association (AHA) has published guidelines for relative levels of blood pressure and their corresponding concern level (figure 1.4) [2]. BP has become an essential in modern medicine to assess cardiovascular health. The AHA reports that "69 percent of people who have a first heart attack, 77 percent who have a first stroke, and 74 percent who have congestive heart failure have blood pressure higher than 140/90 mmHg" [2]. Therefore, high blood pressure is defined as having a systolic blood pressure (SBP) greater than 140 or diastolic blood pressure (DBP) greater than 90 (or having a physician diagnosis you with high blood pressure more than twice) [2]. Hypertension is estimated to be a cause of more than 10 percent of deaths worldwide, earning its title as the silent killer [2].

While HR and BP are central and integrated measures of cardiovascular health, there remains many uncertainties. One or two measurements alone cannot adequately summarize the cardiovascular health of an individual. Simple and noninvasive tests that have normative measures facilitate clinical assessment and are in high demand.

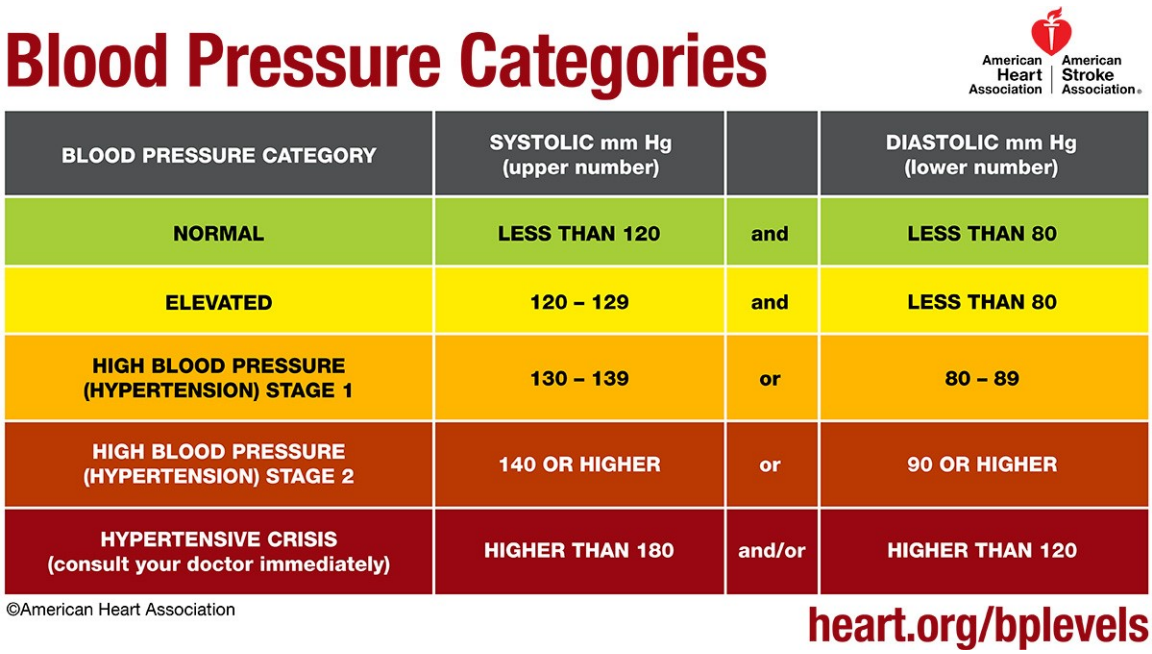

Fig. 1.4 American Heart Association guidelines for blood pressure categories [2].

Many new signal processing measurements have evolved including HRV analysis, which can assess cardiovascular health within minutes using nothing more than ECG.

1.2 Role of the Autonomic Nervous System in Cardiovascular Homeostasis

1.2.1 Branches of the Autonomic Nervous System

The brain and spinal cord make up the CNS, while all other neural tissues make up the peripheral nervous system. In the peripheral nervous system, there are two main divisions: somatic (voluntary actions) and autonomic. The ANS consists of all automatic and non-voluntary functions. There are two main divisions of the ANS: sympathetic and parasympathetic. A third division, the enteric nervous system, is located in the gut and regulates gastrointestinal activity [10, 11]. Its function is considered mostly independent or separate from the sympathetic and parasympathetic

branches and as such is beyond the scope of this thesis. A diagram visualization of the categorical branching of the nervous system is provided (figure 1.5).

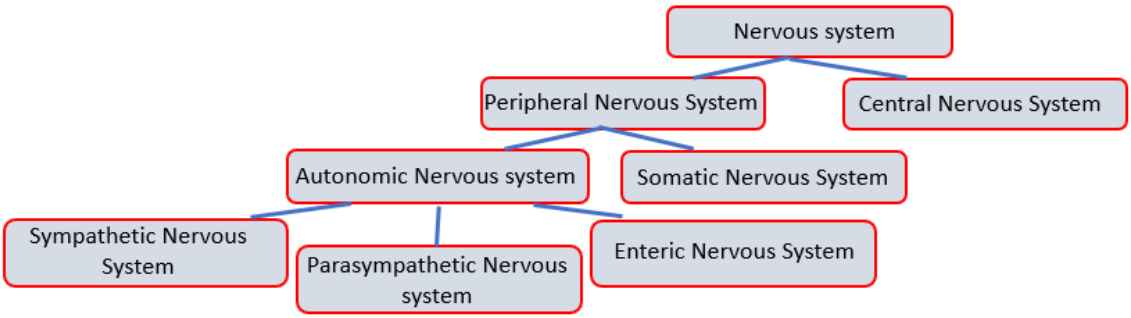

Fig. 1.5 Nervous system diagram.

The sympathetic and parasympathetic divisions of the ANS present a unique function and physiology. The sympathetic nervous system (SNS) is responsible for arousing the body to respond to a situation, while the parasympathetic nervous system (PNS) is responsible for calming the body and restoring its resources. The cooperation of these branches indicates how appropriately the nervous system is functioning and thus is a central concern in assessing cardiovascular health.

1.2.2 Homeostasis and Control in the Cardiovascular System

Homeostasis is a dynamic state of equilibrium and practically defined as the body's inclination toward maintaining a healthy internal environment [11]. To achieve this, the body relies on a large series of feedback pathways that communicate with the CNS and this is schematized in figure 1.6 [8, 11].

These feedback pathways operate at different rates and manifest in many forms including mechanical, chemical, and electrical. The fastest known communication pathways in the body are neurogenic, i.e., electrochemical [8, 11]. These pathways are composed of axons (highly conductive nerve tissue) and can respond to stimulus in less than a second. Other feedback pathways utilize hormonal and slower internal mechanisms (minutes to days) [8]. The rate at which the body needs to operate at in

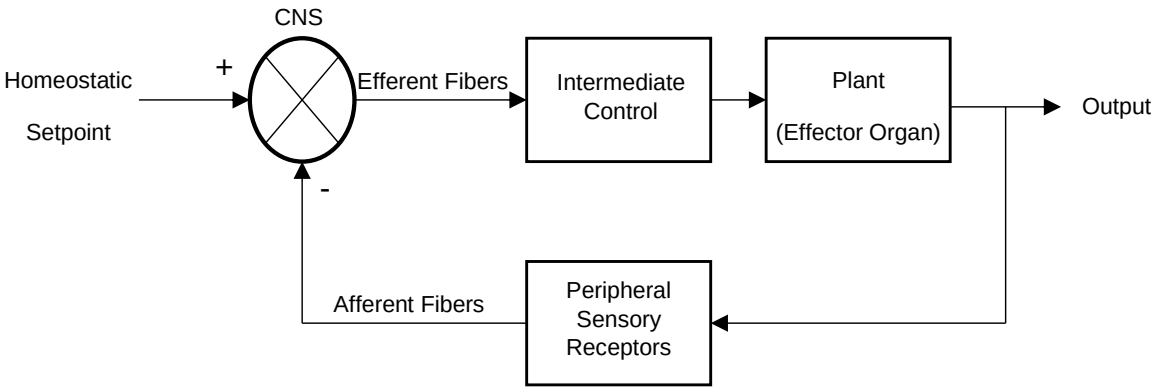

Fig. 1.6 Control system viewpoint of feedback loops in the autonomic nervous system (adjusted from [8]).

any given feedback cycle is reflected by the physical type of pathway utilized in that cycle.

These networks of feedback pathways provide the body with high levels of integrated control. Overall, the pathways sum to form a closed loop negative feedback structure in the CNS [8,11]. The dorsal root and cranial nerve ganglia have numerous sensory fibers that communicate with the CNS, which causes the CNS to generate necessary corrections to return the body to homeostasis [8, 11]. These fibers are the afferent inputs to the CNS, while their correlating effects to the system are the efferent outputs. This constant stream of information going through afferent and efferent channels among all the organs and the CNS creates an on-going oscillation, referred to as sympathovagal balance.

1.2.3 Sympathovagal Balance

The term sympathovagal balance refers to the overall autonomic state the body is in as a result of the influences from the SNS and PNS working simultaneously [12–24]. By functioning together with nearly reciprocal purposes, there is a constant oscillation of the body's autonomic state that is centered around a relative homeostatic plane [8, 11–24].

The simplified end function of the SNS is often to arouse the body, commonly referred to as the 'fight or flight' response. The simplified end function of the PNS is to drive the body back to homeostasis, often referred to as 'rest and digest' [8,10,11]. When either branch changes in activity, the other branch responds, creating a new level of sympathovagal balance [8, 11].

New, relative homeostatic levels can arise from different underlying autonomic states. For instance, someone that is at rest has a significantly different autonomic tone than someone that is performing any form of exercise [16, 22, 25–30]. Exercise actively promotes blood flow through the heart, skeletal muscles, and lungs. When someone is eating, there is more blood flow to the digestive system. During rest, blood flow is focused to the kidneys and gastrointestinal system. These blood flow transitions require significant shifts in ANS. Yet, it can be expected that HR and BP will be at levels appropriately matched to cardiac demand. In other words, the level of energy that is exercised in the SNS and PNS could be relatively low, medium, or very high, but the body can remain in a balanced state [11, 25]. This demands the necessity of being able to evaluate the ANS so that the intricacies of the underlying tone of the ANS can be interpreted accurately.

1.2.4 Clinical Assessments of the Autonomic Nervous System

To assess the ANS and quantify its function, it is necessary to compare a measured variable and compare it to a perturbed one [8, 11, 25]. Analyzing the reaction of the ANS in response to an isolated perturbation allows a specific reflex or feedback pathway to be quantified. In order to stimulate the ANS, numerous tests have been developed over time for use in the clinical setting [25]. These tests fall in one of two categories: mechanical or chemical.

Mechanical assessments of the nervous system aim to promote the natural response of the ANS without introducing any foreign chemical agent. Mechanical interventions can be invasive in some cases, such as the innervation or denervation of nerve tissue

[7, 25, 30]. Less invasive mechanical tests include tilt table, deep respiration, and more [6, 11, 13, 14, 16, 17, 19, 20, 22, 26–29, 31–39]. In each of these tests, one or more variables, such as HR or BP, is perturbed to assess the body's cardiovascular response. For example, the tilt table test involves having a patient flipped upside down on a motorized table while their ECG and BP are constantly monitored. Blood flow to the brain and heart rate are temporarily slowed, which causes a compensatory response in the CVS that can be quantified to diagnose the patient. This is often done to find the cause of a patient's syncope (fainting). It also produces perturbations in HRV and has significant effects on the overall time series of the ECG. Therefore, there is demonstrated efficacy of using HRV as an additional measure of ANS function in the clinical setting [6, 7, 13, 16, 18–24, 27, 29, 32, 36, 38, 40–43]. However, since many factors contribute to HRV, it is necessary to construct more tightly controlled tests where the perturbation in the ANS can be localized to specific feedback pathways, such as the BRx, to limit potential bias in the quantification techniques.

Chemical or pharmaceutical tests of the nervous system aim to promote a response of the ANS without mechanical means. Certain drugs are utilized in a clinical setting for testing the ANS because of their limited risks and high efficacy. These include nitroglycerin, phenylephrine, and others [12, 14, 17, 18, 25, 30, 31, 38, 44–52, 52, 53]. Nitroglycerin is often used during a tilt table test because it induces vasodilation, which reduces BP and can elicit syncope. Phenylephrine is an alpha-adrenergic agonist, meaning it mimics the effects of activating the SNS. It increases HR and BP immediately, forcing the CVS to compensate and bring the system back into balance. However, its powerful drive is not localized just to the BRx when it forces activation of the SNS. This is a common drawback of most chemical tests, and it creates significant variance and uncertainties in data, making it particularly difficult to justify as a robust clinical measurement [7, 17, 18, 47, 48]. Nonetheless, chemical means are effective at activating autonomic perturbations as to assess cardiovascular function.

1.2.5 The Baroreflex – A Rapid Controller of Heart Rate and Blood Pressure

The BRx is the primary negative feedback loop controller in charge of maintaining homeostasis of the CVS [8, 11, 23, 25, 39, 53–56]. Baroreceptors are mechanoreceptors – they respond to physical stretching. When BP changes, it causes the baroreceptors to fire action potentials along axons [8, 11]. These action potentials are afferent information, as they go to the nucleus of the solitary tract in the CNS to be integrated by CNS structures [8]. After integration, the nucleus of the solitary tract sends an efferent drive through sympathetic and parasympathetic efferent nerves. The parasympathetic drive is fast enough to reach the effector organ (the heart) before the next heart beat occurs, allowing it to slow the autonomic pacing cells in the sinoatrial node and decrease the HR in a single heart beat [8, 11, 25, 36, 55].

One of the most useful quantifications of the ANS is baroreflex sensitivity (BRS). BRS is a method that assesses the gain of the BRx [25, 39, 45, 53–56]. BRS is defined as "the change in interbeat interval in milliseconds per unit change in blood pressure" [57]. This is measured in milliseconds per millimeters of mercury. This measurement directly quantifies how fast and by how much the BRx is able to change the HR in response to a given change in BP. BRS requires a patient's ECG as well as their simultaneous BP profile. Techniques like BRS provide useful measurements for quantifying the ANS because of their practical clinical requirements.

1.2.6 The Autonomic Nervous System's Control of Homeostasis

When a problem or perturbation is introduced to the ANS, the disparity between the desired homeostatic plane and the feedback of the target organ are summed in the CNS and to a large extent this sensory integration begins at the level of the nucleus of the solitary tract [8]. This integration quantifies the error in the system (how far away from normal the target organ is). To regain balance, the CNS generates an efferent drive to compensate for the afferent response. However, because any given

perturbation likely effects multiple organs, which are integrative and cooperative, there is never a simple final solution [8, 11].

The SNS and PNS are constantly in a 'push and pull' relationship, causing never ending oscillations in the cardiovascular branch of ANS [11]. This represents a sinusoidal steady state model where relative overall power in the system is maintained.

1.3 Heart Rate Variability

1.3.1 Understanding Heart Rate Variability

Sympathovagal balance directly affects the sinoatrial node, which controls the timing of every cardiac cycle and imparts slight variations between heartbeats in a healthy heart's rhythm (figure 1.3) [13]. Furthermore, the lack of HRV in an individual has been proven to have prognostic value in that there is a strong correlation in ANS rhythmicity and sudden cardiac death [58]. Thus, research into HRV is rapidly expanding, with a recent PUBMED title search of 'heart rate variability' yielding nearly 26000 publications from the last 50 years. Numerous methods for HRV have been developed, but they contain serious caveats that need to be addressed.

1.3.2 Techniques to Quantify Heart Rate Variability

Two main categories exist for quantifying HRV: time domain analysis and frequency domain analysis [14, 17, 19, 24, 41, 42, 59]. In both methods, the objective is to quantify sympathovagal balance. More specifically, the ideal measurement quantifies both the discrete and combined contributions of the SNS and PNS on the sinoatrial node.

Time domain analysis is rooted in measuring and understanding the time series vector of successive heart beats. In analyzing the time period for each heartbeat, there are several trends and correlations that reflect autonomic influence. Some of the most common time domain techniques include RMSSD, SDNN, pNN50, and more

[13, 41]. Each measurement quantifies a behavior or trend of the heartbeat intervals within a short time span. With humans, time domain techniques usually utilize between two and five minutes of ECG data, or approximately 120-300 periods of heart beats [14, 17, 24, 41, 59]. In nearly every time domain measurement technique, the fundamental assumption is that contributions of the SNS tend to increase HR (because its serves to arouse the nervous system), while contributions of the PNS tend to decrease HR (because it serves to restore the system) [17, 30]. This statement is an oversimplification, although it is well understood that these contributions reflect the fundamental mechanisms of the ANS to a certain extent. There are many exceptions to these assumptions, which is in part why frequency domain analysis has also evolved.

Frequency domain analysis aims to quantify the fundamental frequencies of the ANS that are responsible for HRV [13, 17, 21, 24, 41]. Each successive heartbeat has a different period that, when considered with neighboring heart beats and the overall R-to-R time series vector, corresponds to quantifiable frequencies. In order to quantify these frequencies, a Fourier transform is utilized, which fundamentally will transform any time series into corresponding frequencies. In the case of HRV, the objective is to quantify the frequencies coming from the SNS and PNS, respectively. One of the advantages of analyzing HRV in the frequency domain is that different regions of the frequency power spectrum have been demonstrated to be correlated to the sympathetic and parasympathetic branches [13, 17, 21, 24, 41]. There is a defined region of low frequencies (i.e. the low frequency band) that was initially demonstrated to be highly correlated with sympathetic tone. However, more recent studies have suggested that the low frequencies are not reflectively of only sympathetic tone. There is an adjacent region of higher frequencies (the high frequency band) that has been demonstrated to be correlated to parasympathetic tone. By measuring these frequency regions, sympathovagal balance can be quantified.

By assessing the fundamental frequencies of the ANS, frequency analysis quantifies the level of integration and control in the ANS. The generated frequency spectrum reveals not only at what frequencies the mechanisms occur, but also at what magni-

tude each relative frequency is occurring. This significantly extends the opportunity for understanding the underlying mechanisms at work in the ANS and allows for experimental tests of the ANS to be quantified in physiologically specific context. However, while inviting the opportunity for specific quantification of the ANS, the frequency domain methods utilize certain assumptions that bring about potential disadvantages.

It is important to understand and justify the assumptions that are utilized in frequency transformations in the context of the experiment. Some of the most common frequency domain techniques used in HRV analysis are the Fast Fourier Transform power spectral density interpretation (FFT and PSD), AR modeling, wavelet transformations, and the STFT [13, 17, 21]. Each frequency method utilizes one or more unique assumptions when transforming the time domain into the frequency domain. For instance, the FFT and PSD assumes that the transformed time series is both stationary and periodic. Stationarity demands that the initial time series is in steady state, or that any given portion of the series is equivalent to another randomly selected portion. In the time domain, this suggests that the pattern of variance in the time domain is relatively consistent, versus being completely random. The assumption of periodicity implies that the given time series is evenly sampled and is repetitive as a quantifiable function. These assumptions are not necessarily utilized in the other frequency domain techniques, although they do utilize other assumptions. FFT and PSD is utilized as the HRV analysis technique in this thesis, because it is believed that the utilized animals (Sprague-Dawley rat breed) were in cardiovascular homeostasis, which implies stationarity. In order to accomplish this, it was necessary to consider several variables in every animal.

1.3.3 Variables to Consider in Heart Rate Variability

Because the CNS integrates the input of countless variables, it necessary to consider how each variable affects HRV analysis. Variables known to influence HRV

include HR, BP, respiration rate, tidal volume, age, sex, and more [11,19,24,41]. The experimental protocol in this thesis carefully monitors and at least partially controls for all of these variables. For example, the utilized anesthetic, urethane, is believed to not bias the ANS or perturb cardiovascular homeostasis, while still establishing a sufficient depth of anesthesia. With the consideration that there are potentially countless confounding variables in HRV analysis, it is necessary to employ fundamentally robust techniques in analysis, namely consistency. Because every technique has its flaws, being consistent in a measurement method is crucial. In this thesis, the experimental protocol was replicated in every experiment as closely as possible.

1.3.4 Clinical Concerns of Heart Rate Variability Analysis

Demonstrating the validity and usefulness of HRV techniques is essential for them to be considered in the clinical scenario. Thus, one of the main focuses of HRV research in the last few decades has been to demonstrate its robustness in quantifying the ANS in response to a perturbation.

Mechanical techniques have been demonstrated to directly correlate to autonomic activity. Less invasive tests such as the aforementioned tilt table test, as well as highly invasive tests, such as sinoaortic innervation or denervation, have been shown to cause significant effects in HRV analysis [13, 17, 20, 25, 28, 31, 34, 51]. Chemical techniques, such as phenylephrine infusion, also correlate to autonomic activity and have measurable effects on HRV analysis. However, there is significant variance in the data, partially attributable to the caveats of HRV analysis. Regardless of the technique for assessing HRV, research indicates the need to justify HRV analysis based on the context of the experiment.

HRV analysis has been around since 1960s, but no single technique has risen to become the 'gold standard'. This demonstrates a strong underlying concern in studies for how to best utilize and perform HRV analysis. Furthermore, it implies a clear need for establishing a better understanding of how to properly implement this signal processing technique before it can become fully accepted as a robust and practical clinical measure.

1.4 Summary of Thesis Objectives

There are four primary objectives of this thesis.

1. Develop a tool for analysis of HRV capable of quantifying HRV in the presence of selective and sustained electrical activation of the BRx.

2. Using frequency power spectrum of HRV to assess BRx function in male and female rats.

3. Explore potential associations between BRS and HRV.

4. Refine experimental techniques and measurements to establish practical guidelines for future experimental protocols investigating HRV and BRx.

CHAPTER 2. MATERIALS AND METHODS

2.1 Introduction

All animal experimental protocols were authorized by the Institutional Animal Care and Use Committee at the Purdue School of Science for IUPUI (protocol no. 278R). A total of 40 Sprague Dawley Rats were utilized consisting of 26 males (Average Weight: 303 +/- 46.9 g; Average Age: 68.5 +/- 11.5 days) and 14 females (Average Weight: 241 +/- 33.2 g; Average Age: 78.3 +/- 10.7 days). This age range is consistent with previous research in the Schild Laboratory investigating sexual dimorphism of the rat BRx [8]. The rats are old enough to obviate concerns regarding ontogenetic factors that may bias reflex function such as sexual maturity and extent of myelination [8,11] and yet young enough to facilitate dissection of autonomic nerves of the neck. The CVS of the rat is physiologically similar to that of human and exhibits much the same dynamic characteristics of autonomic reflex control of the heart and circulation. Furthermore, unique to rats there exists an anatomically distinct afferent nerve trunk that consists of solely mechanosensory fibers (baroreceptors). Termed the aortic depressor nerve (ADN), these stretch-sensitive afferents convey a powerful parasympathetic drive of the arterial BRx. Recent work in the Schild lab has demonstrated a unique difference in myelinated baroreceptor fiber distribution between male and female rats that significantly augments the baroreflex in females as compared to age-matched males [8]. An overarching hypothesis of this thesis research is that sexual dimorphism may also be apparent in HRV arising from the magnitude and phase of afferent sensory feedback. All animal preparations were consistent with those of earlier research in the Schild lab and only briefly described here [8]. The sole

exception concerned the ADN stimulation protocols which were modified to provide data records of adequate duration and control reference for precision HRV analysis.

2.2 Animal Preparation Protocol

Upon arrival at the vivarium, animals were allowed to accommodate for at least one day before use in an experiment. Following transport to the laboratory, the rat was exposed to the volatile anesthetic isoflurane (Henry Shein) within a sealed induction chamber. Once lightly anesthetized, an intraperitoneal (IP) injection of an anesthetic solution consisting of urethane (200 mg/mL; Ethyl Carbamate 97%, Argos Organics) and alpha chloralose (10 mg/mL; AT, Sigma Life Sciences) was administered (dosage: 0.8mL/100g). This combination of urethane and alpha chloralose has long been shown to provide a stable plane of surgical anesthesia without significantly altering autonomic control of the heart. A surgical plane of anesthesia was considered established when the rat lacked reflex response to a noxious stimulus such as tail and toe pinches.

2.3 Surgery Protocol

The surgery protocol consisted of 3 major stages: 1) tracheotomy, 2) catheterization of the left femoral artery and 3) blunt dissection of the left aortic depressor nerve.

2.3.1 Tracheotomy

A tracheotomy helps the animal to breath which is particularly important as it is unnatural for a rat to be in a supine dorsal recumbent position. A small 1-2 cm midline incision was made on the ventral side of the neck just above the trachea. The underlying musculature was bluntly dissected to provide access to the trachea which was freed from surrounding tissues. A small incision was made in one of the cartilage

rings just below the larynx and a tracheal tube was inserted and secured with suture. The animal was allowed to breath spontaneously while the balance of the surgical protocol was completed. If the animal showed signs of respiratory distress, then a small animal respirator (Harvard Apparatus Model 683) was utilized.

2.3.2 Catheterization of the Left Femoral Artery

Inserting a catheter into the artery allows for continuous recording of arterial pressure. A one-centimeter segment of the left femoral artery was isolated with blunt dissection. The artery was pulled into tension to temporarily stop blood flow. Lidocaine (2%; Henry Schein) was then dripped onto the vessel to relax the arterial smooth musculature, thus dilating the artery which facilitated the entry of the catheter. A small cut was made (1-2 mm) into the artery and the catheter (PE 50; Sublite) was inserted and secured with suture. The catheter was prefilled with heparinized saline (30 U/mL; Sagent Pharmaceuticals). After insertion, the blood pressure transducer (Radnoti, CA) was connected to the catheter.

2.3.3 Isolation and Stimulation of the Aortic Depressor Nerve

Access to the left ADN allows for selective activation of the BRx. Blunt dissection was performed lateral to the trachea. The ADN trunk is about 100 micrometers or less in diameter and lies within the skeletal musculature of the neck. Running parallel between the carotid artery and the vagus nerve and often comingling with a fine sympathetic nerve trunk, the ADN cannot reliably be identified visually. Therefore, a short duration suprathreshold electrical stimulus is applied to the dissected nerve trunk to confirm control of reflex function. A bipolar hook electrode (PBAA0875, FHC) attached to a micromanipulator (M3301R, World Precision Instruments) was used to suspend the ADN and deliver electrical stimulation (continuous pulse train; 50Hz, 5 seconds, 250 microsecond pulses, 2V). A rapid and acute depression of arterial BP (approximately 30-60 mmHg over 5-10 seconds) confirmed the dissected nerve

trunk was the ADN. Following confirmation, the interface with the hook electrode was coated in a mixture of Vaseline and mineral oil, allowing the nerve to remain hydrated and limit interstitial fluid diffusion that would short the electrode contacts.

2.4 Transition Period

Heart rate, BP, and respiration were continuously monitored. Because the experimental protocol is autonomically stressful, a transition period (30 minutes - 2 hours) was often necessary before proceeding with the experimental protocol. This involved waiting until the HR and BP returned to the defined stable range (4-6 Hz and 100 +/- 10 mmHg, respectively).

2.5 Controlling Respiration

Tidal volume and respiration are well known to effect HRV because of the autonomic neural circuitry that underlies RSA [19, 42, 60]. The cyclical acceleration and deceleration of HR produces a frequency peak in the power spectrum at the respiration rate. The respirator (63 breaths per minute, 1.25cc) was used to control the rat's respiration after a natural-breathing baseline of ECG and BP was recorded. A transition period (10-30 minutes) was given for the rat to adjust to the respirator before proceeding to the stimulation protocol.

2.6 Stimulation Protocol

Following a baseline recording of spontaneous respiration, the continuous stimulation protocol was carried out, consisting of 10 minutes of 5 Hz bipolar electrical stimulation (2V regulated, 250 microsecond pulse width) of the left ADN. The protocol was repeated if the animal regained stability after stimulation.

2.7 Timeline and Order of Experiment

A timeline for the experimental protocol is given in Table 2.1.

Table 2.1 Timeline of Experiments

Preparation Step	**Time Required (Range in Minutes)**
Anesthetic Preparation	30
Animal Preparation Protocol	30-60
Surgery Protocol	60-195
Stabilization Period	30-120
Stimulation Protocol	70-200
Clean Up	30
Total	250-635

2.8 Data Collection

There were three main segments during which the HR and BP were recorded for analysis with the HRV algorithm:

1. A baseline recording taken during the stabilization period during which the animal was breathing spontaneously (26 males; 14 females).

2. A baseline recording taken after the animal adjusted to the respirator, immediately preceding the stimulation of the ADN (3 males; 3 females).

3. A stimulation recording taken during the electrical stimulation of the ADN (3 females).

2.9 Inspection of ECG

ECG abnormalities can have significant effects on HRV [13, 17, 19, 33]. Abnormalities include any irregular heartbeats that are caused by an underlying problem with

the heart's electrophysiology. For example, there are arrhythmias that arise because the heart has become dissociated from the sinoatrial node [61]. This can cause the heart to lose active ANS pacing and a healthy and controlled rhythm. This has been shown to have several repercussions in the ANS. For example, atrioventricular dissociation is a condition where the sequential pathway between the atria and ventricles is temporarily lost [61]. This results in the ventricles contracting independently of the sinoatrial node. This can cause problems in the cardiovascular system's ability to meet hemodynamic demands. As a precaution against such data bias, each ECG record was visually inspected to ensure that no apparent abnormalities were recorded. If any abnormalities were found, the data was not used. Relatively common (about 5-10% of ECGs inspected in this thesis) abnormalities included premature ventricular contractions, indicated by an R wave that occurs sooner than it should.

2.10 Development of Heart Rate Variability Analysis Algorithm

MATLAB 2019a was used to build the heart rate variability analysis algorithm utilizing Welch's method and power spectral density conversion. This algorithm involved 10 major steps (figure 2.1), further detailed below.

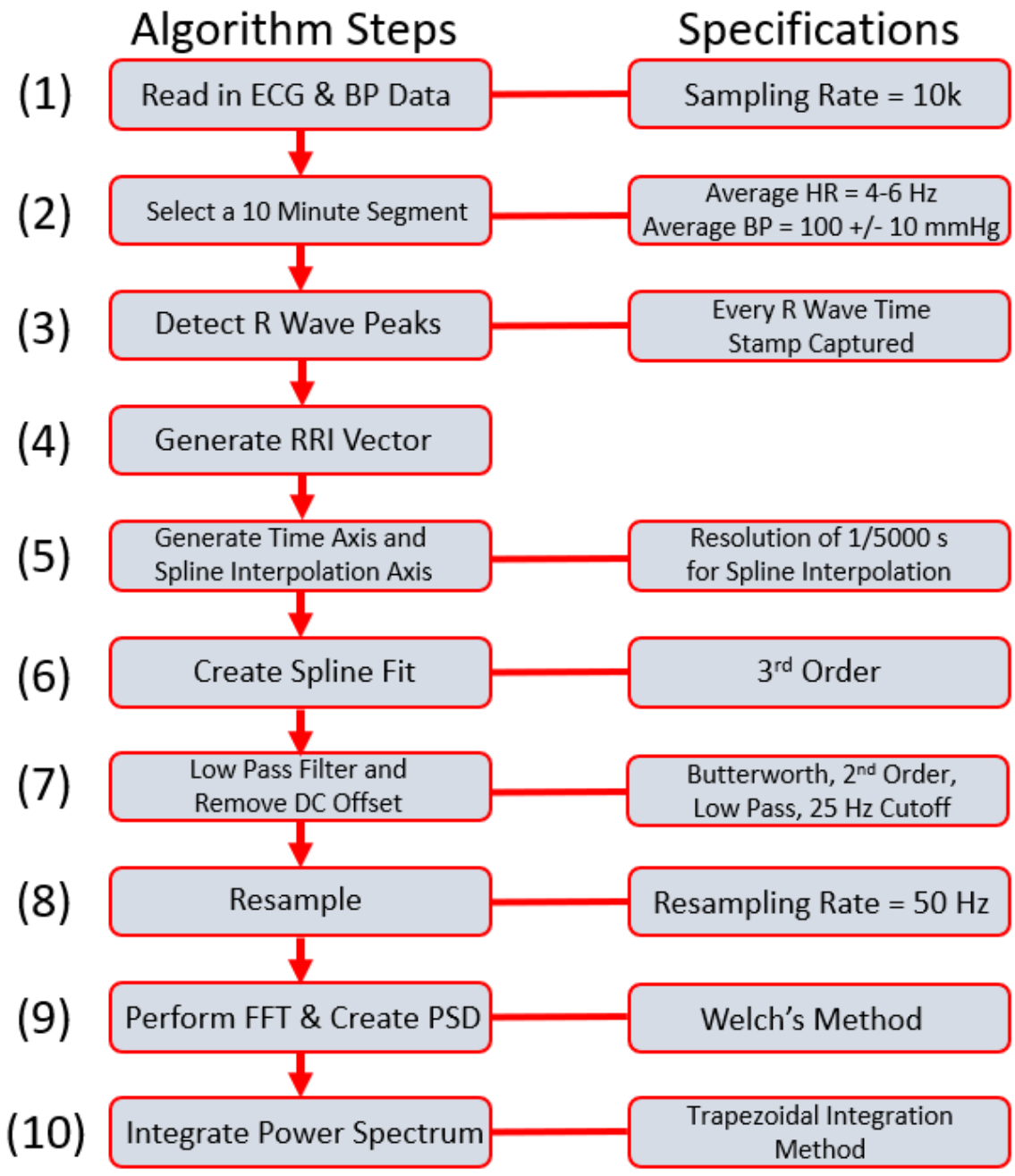

Fig. 2.1 Block diagram of the ten steps used to create the HRV algorithm. Specifications meet or exceed those established as acceptable for HRV [19].

1. Reading in the ECG Data - The ECG, BP, and stimulation data were recorded with a sampling rate of 10k using a proprietary software package (Mr. Kick) for easy import into MATLAB. HRV analysis assumes that the timing of each heartbeat (the R wave) is detected exactly. A sampling rate of two hundred times the heart rate is acceptable for HRV [19]. A higher sampling rate has no disadvantages. The utilized sampling rate of 10k is approximately two thousand times the heart rate of a rat, satisfying this requirement.

2. Selecting a Ten-minute Segment of Data - Data profiles could be as long as 120 minutes. The entirety of each data set was inspected to find the most stable ten-minute portion. Mean HR was required to be 4-6 Hz and mean BP was required to be 100 +/- 10 mmHg. Because the BP profile had considerable variance in each surgery with respect to its detected peak to peak amplitude (resulting from cyclic systolic and diastolic transitions), the DC average was used to assess stability (figure 2.2). Respiration rate during that segment was measured by performing an FFT on the BP profile (figure 2.3). The respiration rate was required to be 1+/- 0.4 Hz. Two to five minutes of data are typically used for HRV analysis in human and rats [14,17–19,30,47,48]. Because Welch's method is utilized for HRV analysis in this thesis, ten-minute segments were selected to (a) verify animal stability, (b) increase signal resolution, and (c) mitigate any potential signal-processing noise. Further explanation is given below.

   (a) If an animal is stable for a ten-minute segment, then it is a strong justification that the signal is stationary.

   (b) Approximately 3000 heartbeats (assuming 5 Hz HR) are contained within ten minutes, compared to half or less than half that many in a two to five-minute segment. This allows the FFT resolution (proportional to 1/number heartbeats) to be much better in preparation for accurate integration of the power spectrum.

(c) Any signal processing errors (such as arbitrary start and stop times) are attenuated proportionally to the length of the data in a FFT.

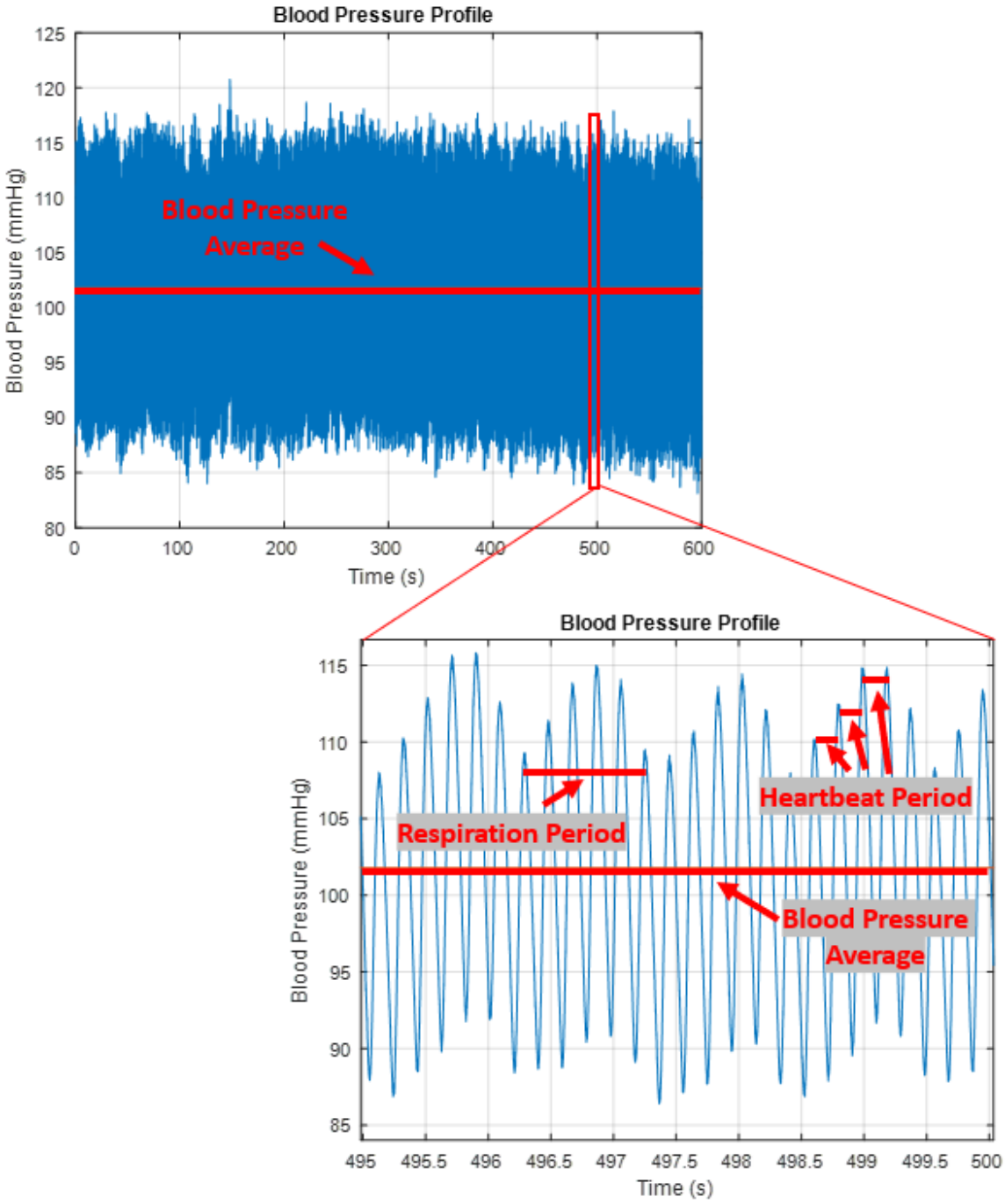

Fig. 2.2 Typical blood pressure profile recorded during a natural breathing baseline in a male rat. The systolic and diastolic transitions (lower graph) varied significantly in experiments, so the DC offset was used to quantify an average.

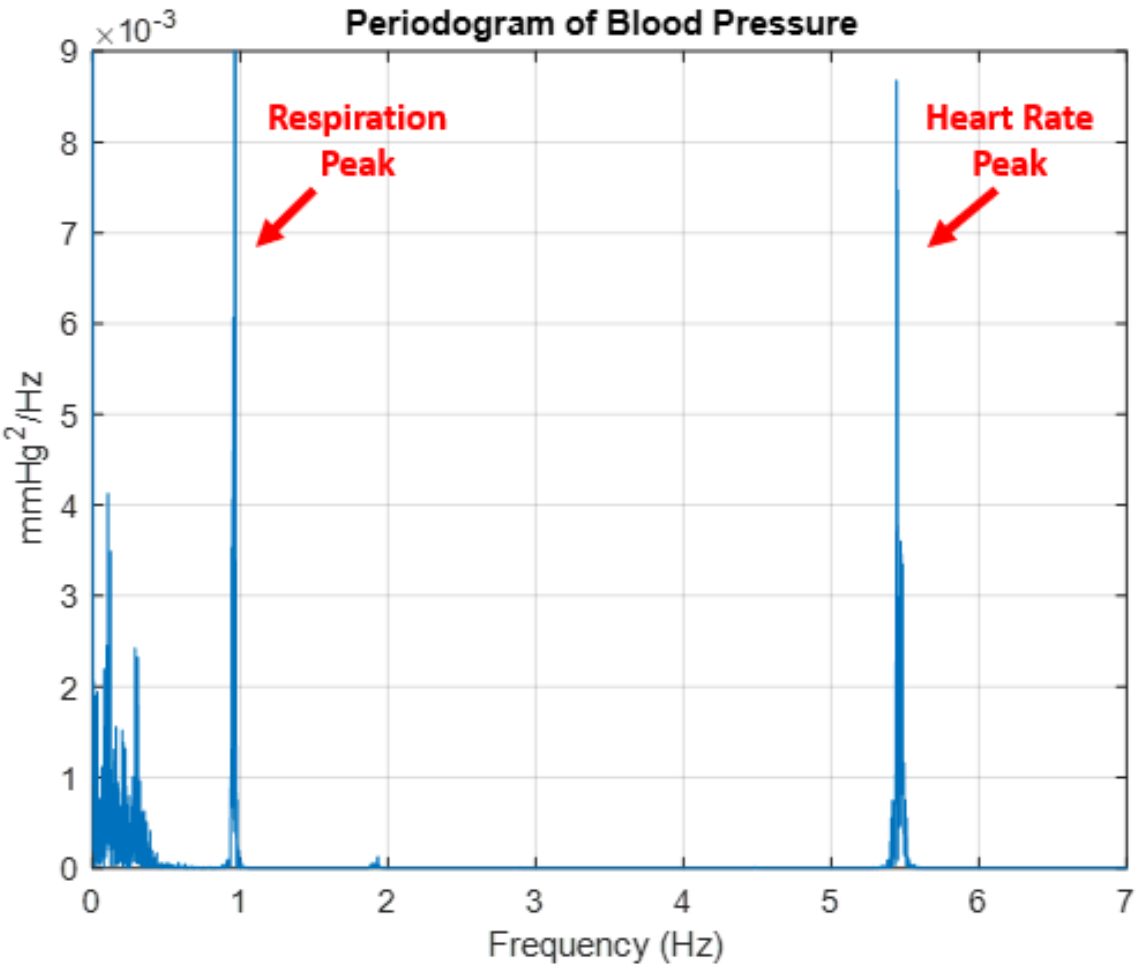

Fig. 2.3 Typical power spectrum of a blood pressure profile taken from a male rat. Respiratory sinus arrhythmia causes a sharp peak to occur that indicates the animal's respiration rate.

3. Detecting ECG R Peak Locations with Windowing - The findpeaks windowing toolbox was utilized to locate the time stamps of every R wave. In addition to the basic local maxima that is utilized in this function, three more criteria were used: minimum peak distance, minimum peak prominence, and minimum peak height. Minimum peak distance varied from 100 to 150ms. Minimum peak prominence varied from 0.15 – 0.8 V. Minimum peak height varied from -10 to 2 V. In 90% of the ECG profiles, minimum peak distance was 150ms, minimum peak prominence was 0.15 V, and minimum peak height was -1 V. In some cases, more uniquely tethered parameters were required. Heart rate variability only considers the time locations of the R peaks in an ECG profile. Therefore, any ECG that had distinguishable R waves could be used (figure 2.4).

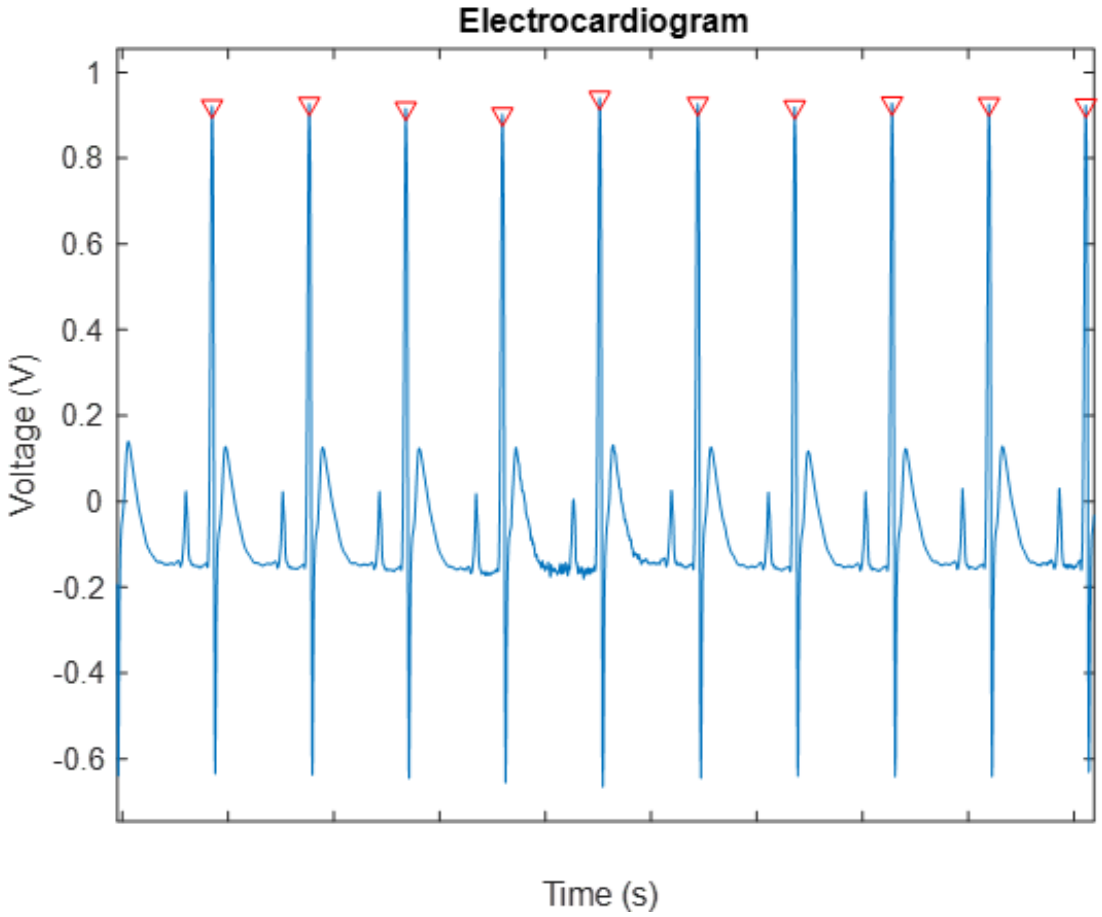

Fig. 2.4 Example ECG taken from a male rat. The algorithm marks the maximum of each R wave and collects the associated time stamps, necessary for generating the RRI time series vector.

4. Generating RRI Vector - After collecting the time stamp of every R wave, the RRI vector was generated by finding the difference between every adjacent R wave (figure 2.5). For instance, the first RRI vector point was the time stamp of the second R wave subtracted by the time stamp of the first R wave. The second point was the 3rd R wave subtracted by the 2nd R wave, and so on.

Fig. 2.5 Demonstration of marked R waves used to generate RRI vector.

5. Generating Averaged Time and Spline Interpolation Axes - To satisfy the periodicity requirement of an FFT, the to-be transformed function must be periodic and evenly sampled. To fulfill these requirements, the most popular method is to perform spline interpolation and resampling [19]. A reference axis and new arbitrary resolution axis need to be created to perform spline interpolation in MATLAB. In this case, the arbitrary axis is time. The reference time axis was calculated by averaging the time stamps between every two successive R waves (figure 2.6). The new arbitrary axis was created with a starting point of 0 and an endpoint equal to the last averaged time stamp value of the RRI vector, with a resolution of 1/5000 s.

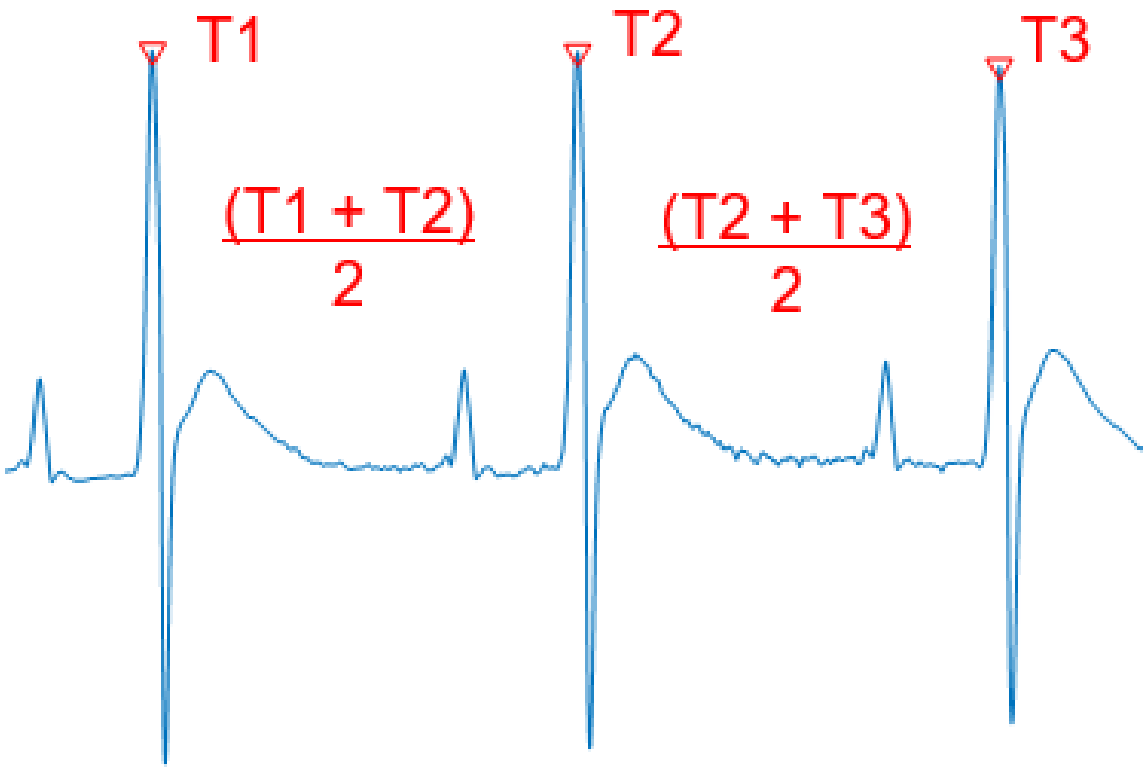

Fig. 2.6 Demonstration of marked R waves used to generate averaged time axis.

6. Creating a Spline Fit to the RRI vector - MATLAB's spline function is utilized for interpolation to produce a 3rd order spline of the RRI vector (figure 2.7). This function uses the generated time and RRI vectors to interpolate the RRI vector with the resolution of the spline interpolation axis.

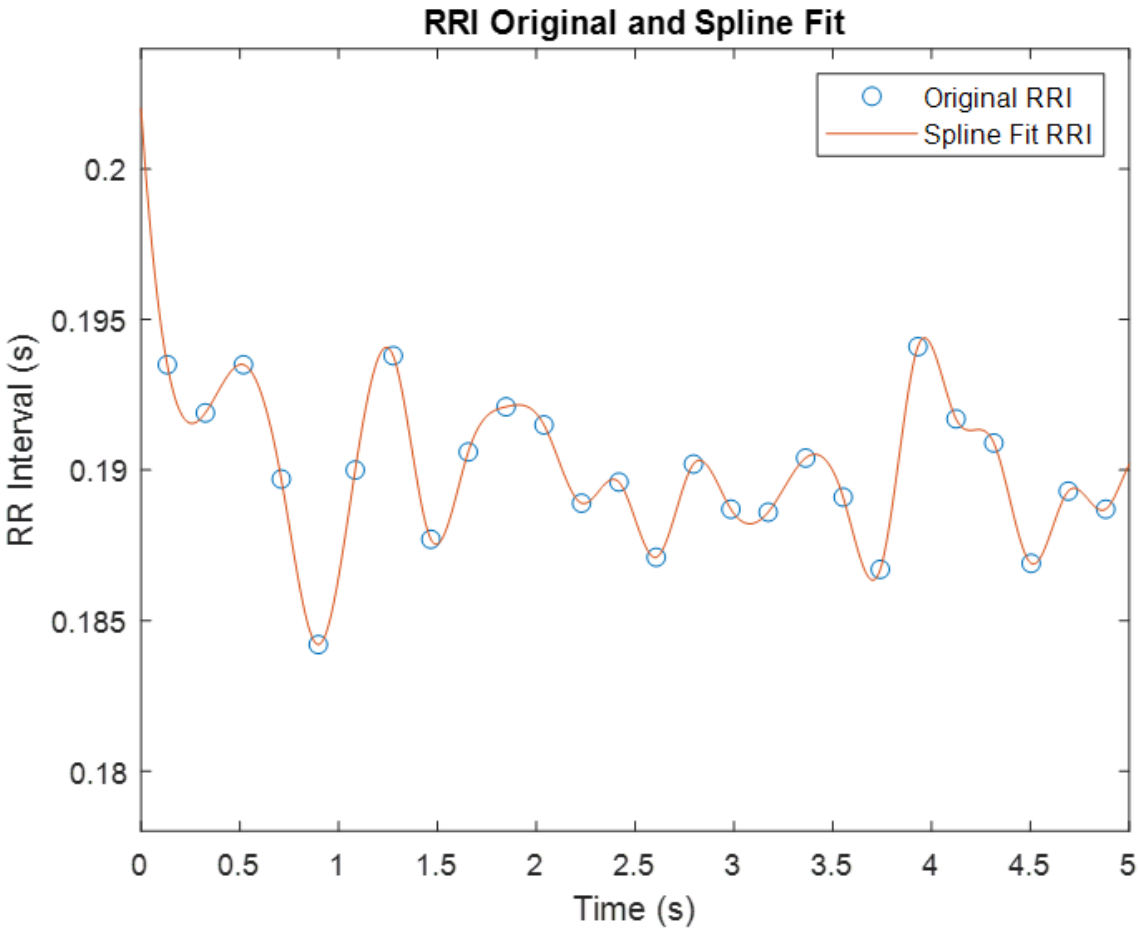

Fig. 2.7 Demonstration of high resolution 3rd order spline fit that interpolates the original RRI vector (5 second window).

7. Low Pass Filtering and Removing DC Offset - To prevent possible signal aliasing, the interpolated RRI is run through a 2nd order low pass Butterworth filter with 25 Hz cut off frequency. Also, the DC component is subtracted to eliminate the zero-frequency peak. The DC component represents the average HR in this case. The variability around the average HR is the focus of HRV analysis, thus it is appropriate to get rid of the DC signal which can be interpreted as unwanted signal noise.

8. Resampling the Interpolated RRI Vector - A loop extracts every 100th point from the interpolated RRI vector, starting with the first point. By extracting every 100th point of a signal with a 5000 times enhanced resolution, the signal is resampled at a rate of 50 (5000/100) Hz. The new interpolated and resampled vector is approximately 30,000 points, which will provide a high resolution periodogram.

9. Performing FFT and Generating Power Spectrum - Welch's method is a modified approach for generating spectral density approximations. Welch's method is computed using the Pwelch function. It splits a signal into as many segments as possible, up to a maximum of 8 (approximately 30,000/8 points in each segment), with 50% overlap. Each segment has a Hamming window applied to it to reduce high frequency noise. The periodogram is then calculated for each segment, and each of the periodograms is averaged to generate one final periodogram. By averaging periodograms, signal noise (inconsistencies between overlapping segments) is attenuated. The power spectrum is computed from the square of the averaged periodogram. This transitions the signal from units of $s/\sqrt[2]{Hz}$ to s^2/Hz.

10. Integrating the Power Spectrum - MATLAB's trapz function is used to calculate the total power s^2 within a frequency band on the power spectrum. This function calculates the integral of the specified region using the trapezoidal method.

2.11 Analysis of Frequency Bands

In the PSD integration technique, certain adjacent frequency bands are defined and the power in each is integrated for comparison. In humans, these frequency divisions are commonly defined as being in a high frequency (HF) band of 0.4 Hz to 0.15 Hz and a low frequency (LF) band of 0.15-0.04 Hz. The high frequency band indicates parasympathetic tone, and the low frequency band indicates sympathetic tone (as aforementioned, the low frequency band is a less certain measure). As the fundamental HR is higher in rat, the frequency bands are expanded proportionally. The rat's low and high frequencies are contained within 0.2-5 Hz [22, 29, 36, 37, 45, 58, 62–64]. In this thesis, the high frequency band is defined as 0.6 – 2.4 Hz and the low frequency was defined as 0.2-0.6 Hz (figure 2.8) which are consistent with previous literature [19, 58, 63].

2.12 Respiratory Peak Analysis

Respiratory peak analysis takes advantage of respiratory sinus arrhythmia. The respiration frequency is defined as the center frequency (fc), a symmetrical tolerance band (α) on either side of it is defined and that region is integrated [42, 60]. This is represented as total power equals fc +/- α (figure 2.9). The value of α was set to 10% and 5% of the amplitude of the respiration peak (e.g. 1 Hz respiration frequency would be represented with 1 +/- 0.05 and 1 +/- 0.1 Hz integration band). These values were chosen so that the respiration peak would always be fully included within the measurement in every data set.

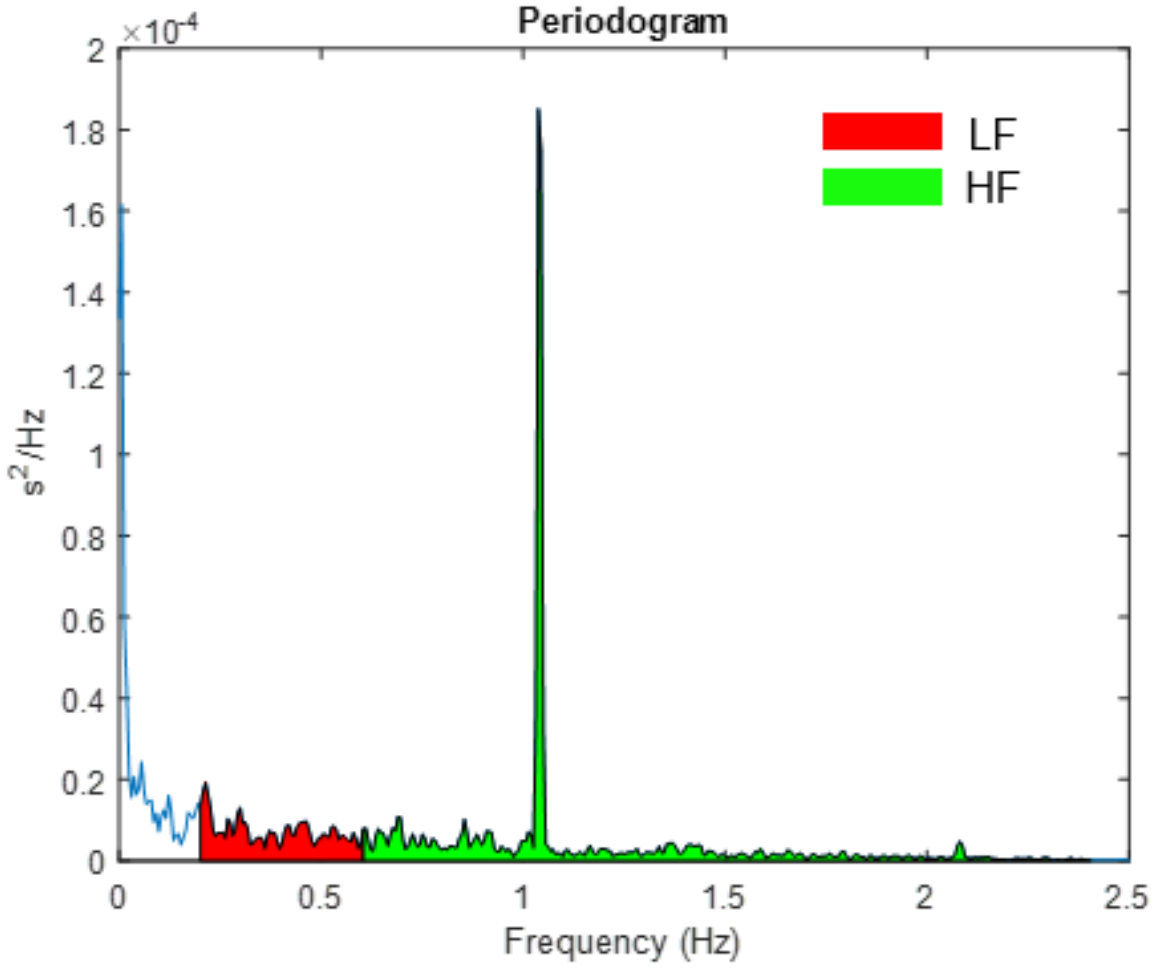

Fig. 2.8 Typical power spectral density graph with low frequency (red) and high frequency (green) regions.

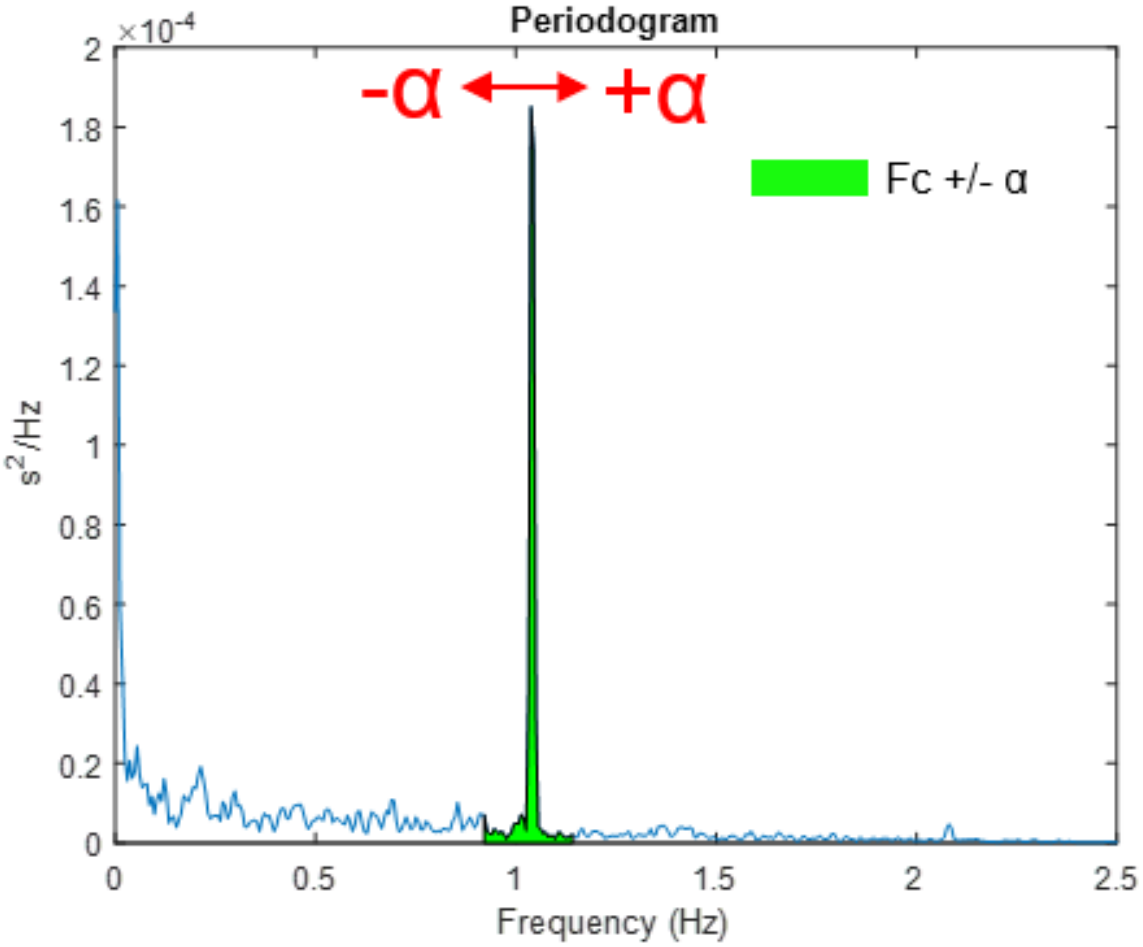

Fig. 2.9 Typical power spectral density graph used in respiratory peak analysis where the respiration frequency band is integrated according to fc +/- α.

2.13 Heart Rate Variability Quantification

The power spectral density-based measurements considered for analysis are listed below. These measurements were chosen because they are commonly utilized in HRV analysis for rats and humans [13, 14, 18, 19, 21, 42, 47, 60].

1. High frequency band absolute power – the total energy obtained from integrating the defined high frequency band of 0.6-2.4 Hz

2. Low frequency band absolute power – the total energy obtained from integrating the defined low frequency of 0.2-0.6 Hz

3. Normalized low and high frequency powers – the total energy in the low and high frequency band when normalized by dividing by the signals total energy contained in both bands (normalized to 100%)

4. Respiratory Peak Analysis – the total energy in the frequency band defined by the respiration peak as the center frequency with a given symmetrical tolerance based on the frequency of the respiration peak, represented by fc +/- α

By comparing the results of each technique to the context of the experimental protocol, the efficacy of each method was assessed.

2.14 Baroreflex Sensitivty Analysis

The objective of BRS analysis is to quantify the entirety of BP control system with one numerical value. Although this is a great simplification, it provides significant information about the ANS. The slope method was utilized to calculate BRS. A series of two consecutive ascending and descending RRI and paired BP values were collected during respirator controlled breathing baseline just before stimulation. These were compared to similar measurements taken from near the end (9 minutes in) of the immediately following stimulation. Linear regression analysis was performed on these

values to generate a BRS value. This produced positive (ascending) and negative (descending) BRS values.

2.15 Statistics

Statistical data analysis and representation were performed using OriginLab 2019b software. T tests with the unequal variance assumption were utilized for comparing males and females. Paired t tests were utilized to compare the respirator baselines with paired stimulations. P values of less than 0.05 were defined as significant.

CHAPTER 3. RESULTS

3.1 Introduction

The overarching objective of this thesis is to use HRV to quantify the ANS during selective activation of the BRx depressor response. It was hypothesized that the previously assessed sexual dimorphism in selective activation of the BRx depressor response could be quantified with HRV. The null hypothesis is that there is no quantifiable association between selective activation of the BRx and HRV. Two commonly used algorithms for HRV were built in MATLAB: frequency band and respiratory peak analysis. These algorithms were used to generate periodograms of RRI vectors. Frequency bands in the periodograms were integrated and compared to assess differences in autonomic tone during spontaneous breathing, controlled breathing, and stimulation of the ADN. Another objective was to compare HRV and BRS. The utilized frequency domain methods for HRV were compared to slope method measurements for BRS during chronic stimulation of the ADN to see if a precise correlation existed between HRV and BRS values.

3.2 Assessing Baseline Stability

Because studies have indicated that differences in baseline stability may be the cause of differences in nearly identical HRV studies [14, 17, 18, 47, 48], the accepted range of baseline parameters for HR and BP was highly restricted. Consistent with a previous Schild lab study [8], the average resting BP was 100.08 +/- 5.46 mmHg

and 100.85 +/- 4.37 mmHg for males and females, respectively. The average resting HR was 5.34 +/- 0.60 Hz and 5.23 +/- 0.41 Hz for males and females, respectively.

3.3 Research Aims

Aim 1: To quantify autonomic tone during selective activation of the BRx using HRV analysis.

Aim 2: Exploring correlations between HRV and BRS.

3.4 Aim 1: Quantifying Autonomic Tone using Heart Rate Variability

Use of Welch's method for HRV analysis was designed using existing algorithms and signal processing techniques in MATLAB. This generated high resolution periodograms from ten-minute ECG profiles. The 0.2 – 0.6 Hz (figure 3.1: red) LF region and 0.6-2.4 Hz (figure 3.1: green) HF region were integrated to produce a total power measurement. Since factors contributing to frequencies below 0.2 Hz (VLF band) are not well understood, the VLF band was not considered in analysis.

The data in figure 3.1 is the periodograms from six rats collected during spontaneous breathing. The animals were believed to be stable based on their HR, BP, and respiration rate (table 3.1).

Table 3.1 Animal Stability Parameters and Frequency Band Powers for Figure 3.1

Animal	**Mean HR** (Hz)	**Mean BP** (mmHg)	**Respiration** (Hz)	**LF Power** (s^2)	**HF Power** (s^2)
Male 1	5.44	99.7	0.96	1.61E-07	5.86E-07
Male 2	5.61	98.9	0.85	2.36E-08	2.36E-07
Male 3	6.03	100.0	0.95	3.25E-08	1.23E-07
Female 1	4.91	96.0	0.71	3.65E-07	2.35E-06
Female 2	5.60	101.6	0.77	4.32E-07	4.11E-07
Female 3	5.50	99.0	0.95	4.27E-08	1.69E-07

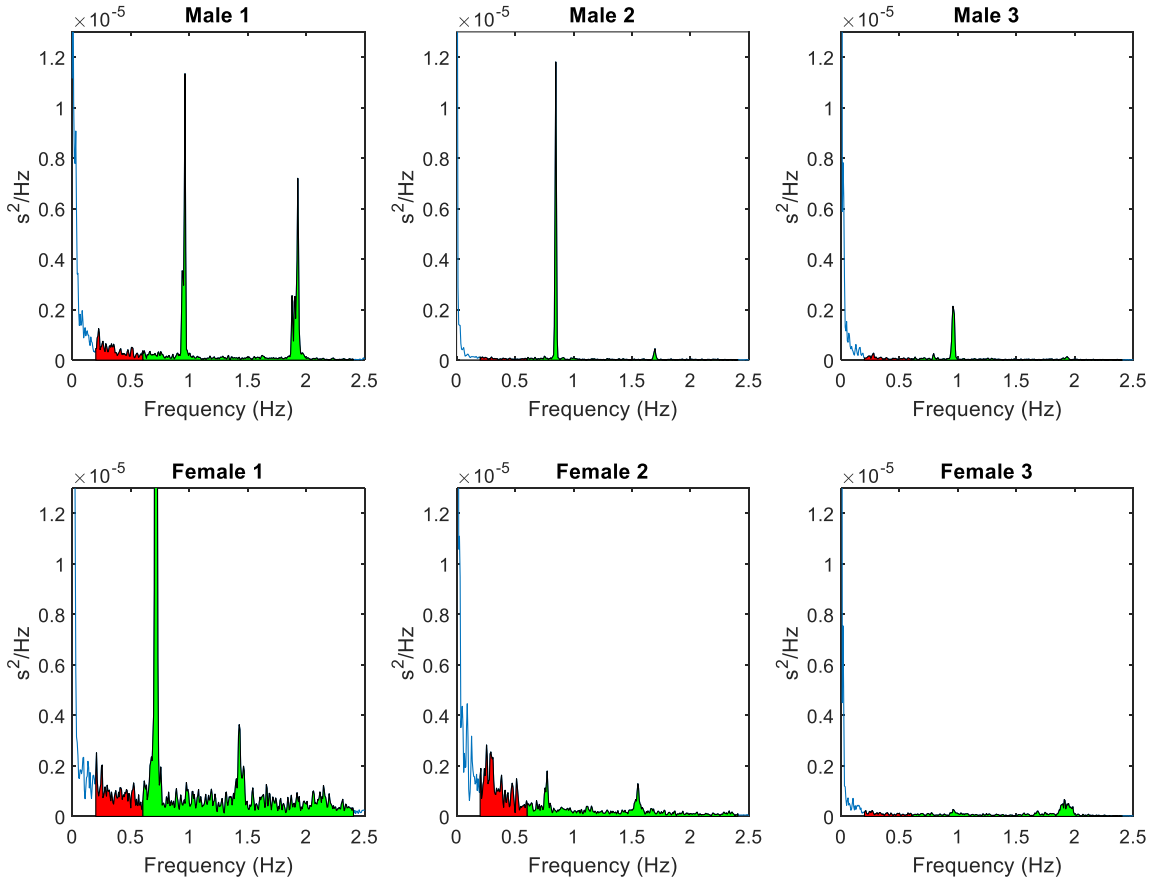

Fig. 3.1 Periodograms from 3 male and female rats recorded during a spontaneous breathing baseline analyzed with frequency band method.

The first analysis looked at only baseline recordings taken during spontaneous breathing. Even with very similar resting heart rates, BP, and stable respiration rates, the animals had a wide range of LF and HF total power. Furthermore, these power differences resulted from different underlying frequencies (figure 3.1). The total power averages from all baseline recordings during spontaneous breathing were compared (figure 3.2). There was no significant difference in mean LF power (p=0.41). There was also no significant difference in mean HF power (p=0.17), although males had a 63% higher mean power.

Given this lack of significance, the stability of the animals was further considered based on ECG histogram type. Specifically, in addition to highly stable HR, BP, and respiration rate, only animals with apparent gaussian ECG histograms were considered (which will be referred to as gaussian data in this work), because a non-gaussian ECG histogram can be indicative of a lack of stability [4]. This reduced n = 26 to n = 9, and n = 14 to n = 6, for males and females, respectively. Even with this gaussian criteria, there was still no significant difference in the LF or HF bands between males and females (figure 3.3). Because the substantial variance was suspected to contribute to the lack of significance, the coefficients of variation (SD divided by the mean) were compared (table 3.2). The coefficients of variation decreased in every measurement in the gaussian data set compared to the non-gaussian data set, which correlated to a smaller p value. In the gaussian data set, the differences in males' and females' HF power was marginally insignificant (p = 0.052).

Because the absolute measures of frequency bands lacked significance regardless of the added filter for a gaussian ECG histogram, normalization that was consistent with literature [13, 14, 18, 19, 21, 37] was performed by defining the total power as the sum of the power in LF and HF bands and dividing each band by the total power. This resulted in the sum of the normalized LF and HF bands equaling one (figures 3.4, 3.5). With this normalization, no significant difference between males and females was seen in the LF (p=0.26) or HF (p=0.26) bands.

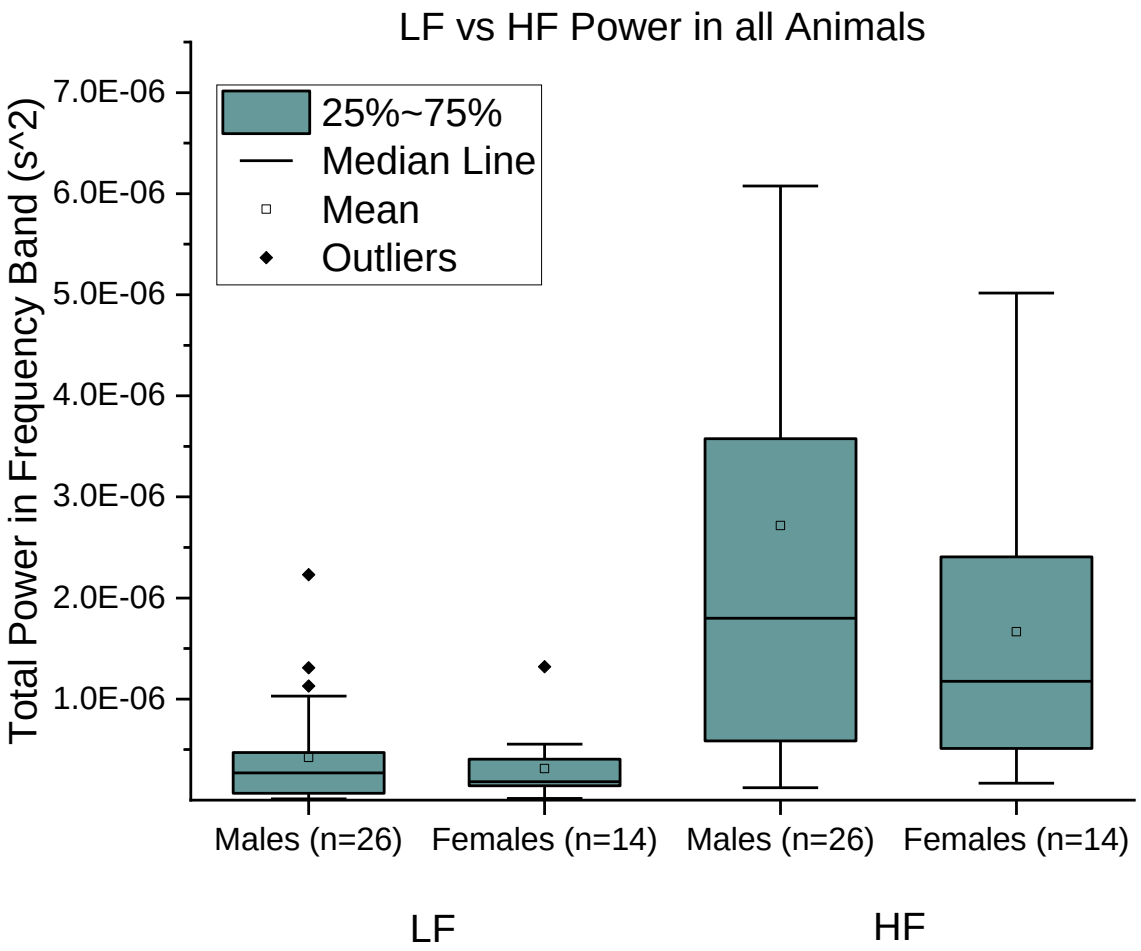

Fig. 3.2 Comparing LF and HF total power for 10 minutes of ECG data during spontaneous breathing baseline. Animals are not discriminated based on ECG histogram distribution type. Mean LF and HF power was higher in males (n=26) than females (n=14). Integrated total powers (mean +/- SD, units are s^2): Male LF power = 4.22 +/- 5.16 E-07. Female LF power = 3.12 +/- 3.31 E-07. Male HF power = 2.71 +/- 3.31 E-06. Female HF power = 1.66 +/- 1.46 E-06.

Following the procedure done with absolute measures, the normalized data sets were further restricted to gaussian data. In the gaussian data, no significant difference between males and females was seen in the normalized LF (p=0.12) or HF (p=0.12) bands. There was no correlation between coefficients of variation and p values (table 3.3), but this is because the utilized normalization technique produces an equivalent

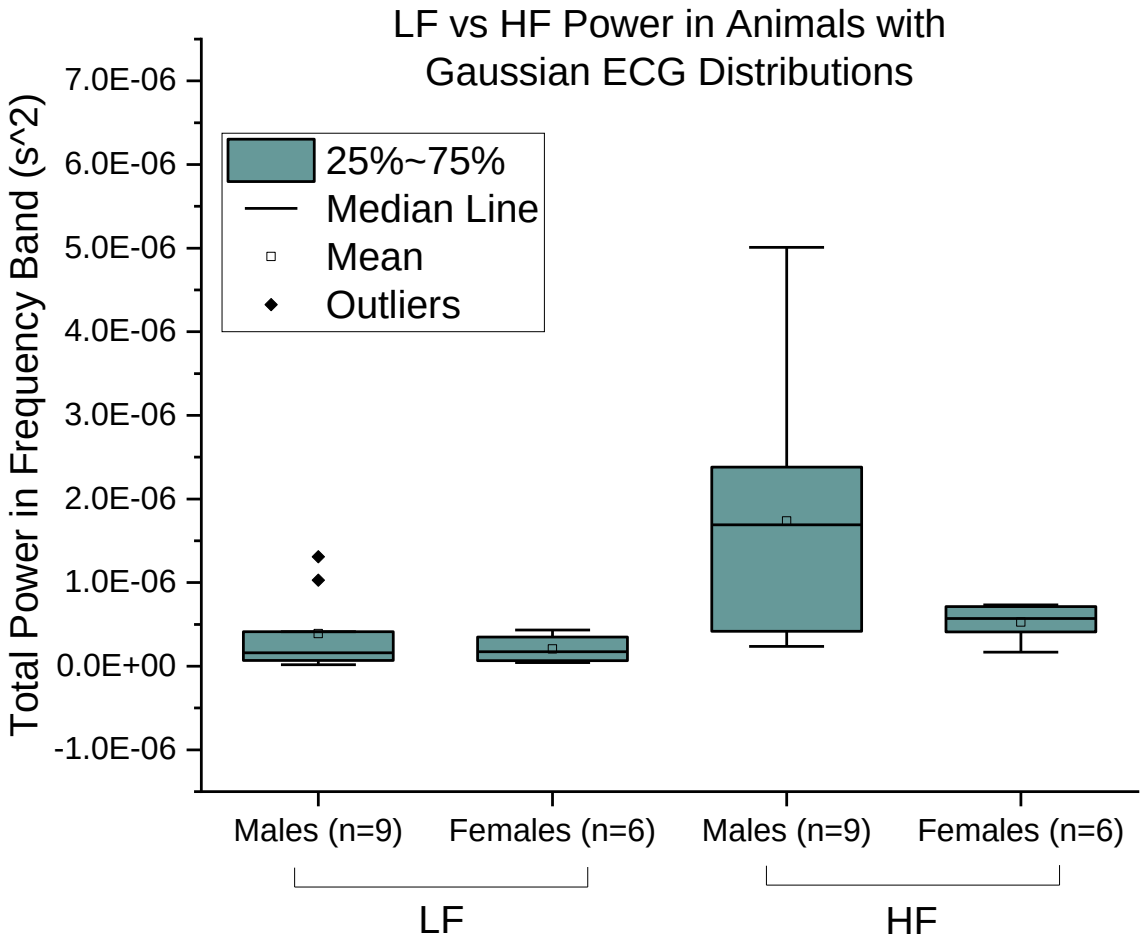

Fig. 3.3 Comparing LF and HF total power for 10 minutes of ECG data during spontaneous breathing baseline. Only animals with an apparent gaussian ECG histogram distribution are included. Mean LF and HF power was higher in males (n=9) than females (n=6). Integrated total powers (mean +/- SD, units are s^2): Male LF power = 3.88 +/- 4.71 E-07. Female LF power = 2.05 +/- 1.54 E-07. Male HF power = 1.73E-06 +/- 1.59 E-06. Female HF power = 5.28 +/- 2.14 E-07.

p value. Normalizing the data decreased significance and increased relative variance in the data.

Table 3.2 Comparing Coefficients of Variation to P values for Males and Females

ECG Histogram Distribution	**Sex**	**Frequency Band**	**Coefficient of Variation**	**P Value**
All (figure 3.2)	Male	LF	1.22	0.41
	Female	LF	1.06	
All (figure 3.2)	Male	HF	1.22	0.17
	Female	HF	0.87	
Gaussian (figure 3.3)	Male	LF	1.21	0.30
	Female	LF	0.75	
Gaussian (figure 3.3)	Male	HF	0.91	0.052
	Female	HF	0.40	

Table 3.3 Comparing Coefficients of Variation to P values for Males and Females with Normalized Frequency Bands

ECG Histogram Distribution	**Sex**	**Frequency Band Normalized**	**Coefficient of Variation**	**P Value**
All (figure 3.4)	Male	LF	0.46	0.26
	Female	LF	0.70	
All (figure 3.4)	Male	HF	0.06	0.26
	Female	HF	0.14	
Gaussian (figure 3.5)	Male	LF	0.50	0.12
	Female	LF	0.53	
Gaussian (figure 3.5)	Male	HF	0.08	0.12
	Female	HF	0.19	

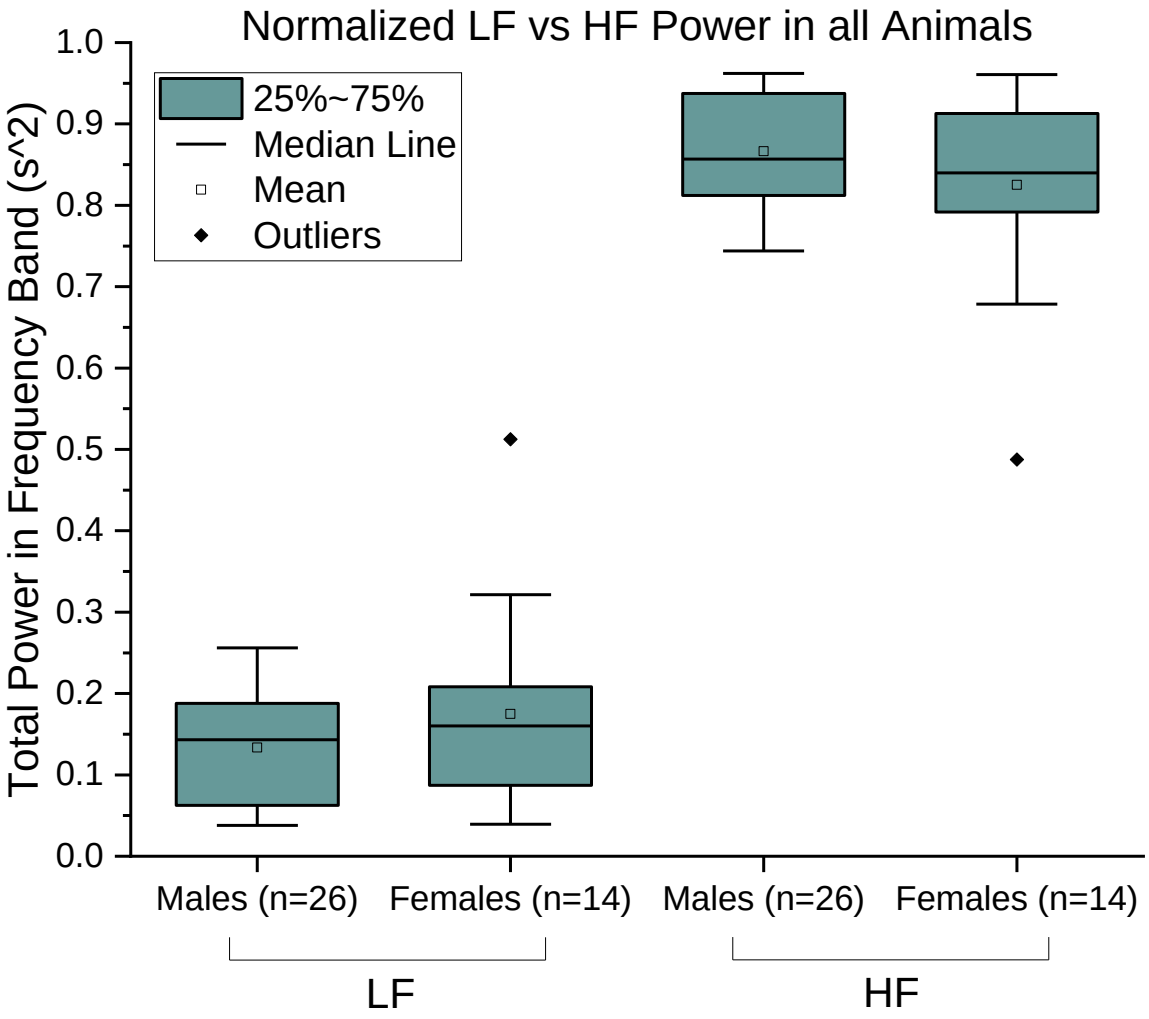

Fig. 3.4 Comparing normalized LF and HF total power for 10 minutes of ECG data during spontaneous breathing baseline. Animals are not discriminated based on ECG histogram distribution type. Mean normalized LF power was higher in females (n=14) than males (n=26). Mean normalized HF power was higher in males (n=26) than females (n=14). Integrated total powers (mean +/- SD, units are s^2): Male LF power = 0.13 +/- 0.06. Female LF power = 0.17 +/- 0.12. Male HF power = 0.86 +/- 0.06. Female HF power = 0.82 +/- 0.12.

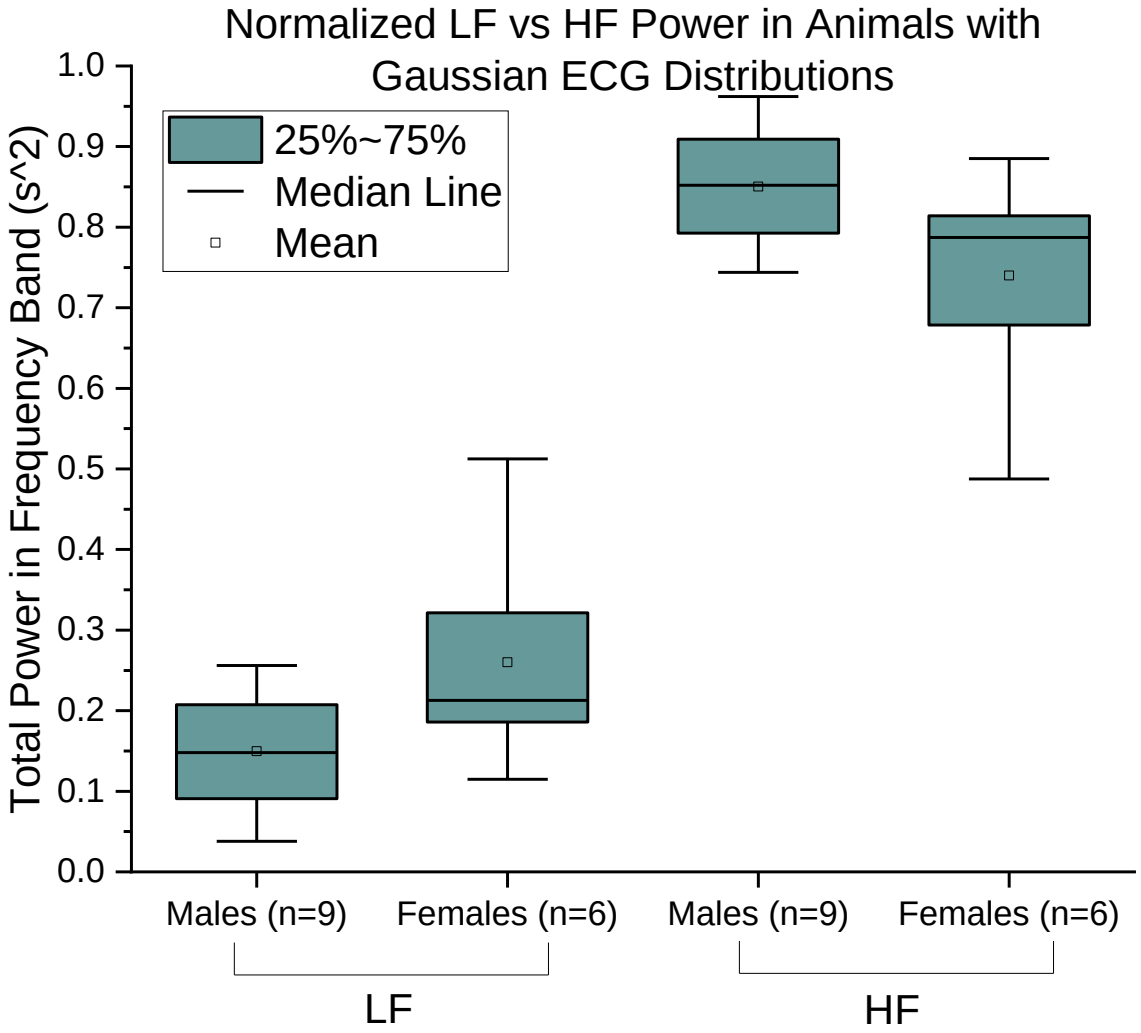

Fig. 3.5 Comparing normalized LF and HF total power for 10 minutes of ECG data during spontaneous breathing baseline. Only animals with an apparent gaussian ECG histogram distribution are included. Mean normalized LF power was higher in females (n=6) than males (n=9). Mean normalized HF power was higher in males (n=9) than females (n=6). Integrated total powers (mean +/- SD, units are s^2): Male LF power = 0.14 +/- 0.07. Female LF power = 0.26 +/- 0.14. Male HF power = 0.85 +/- 0.07. Female HF power = 0.73 +/- 0.14.

Because the normalization method did not demonstrate any significance, the respiratory peak (fc) analysis method was utilized to assess the power density spectrums. A symmetrical (α = 10% and 5%) band centered on the respiratory peak was integrated (figure 3.6: green; α = 10%) to obtain a total power value (table 3.4).

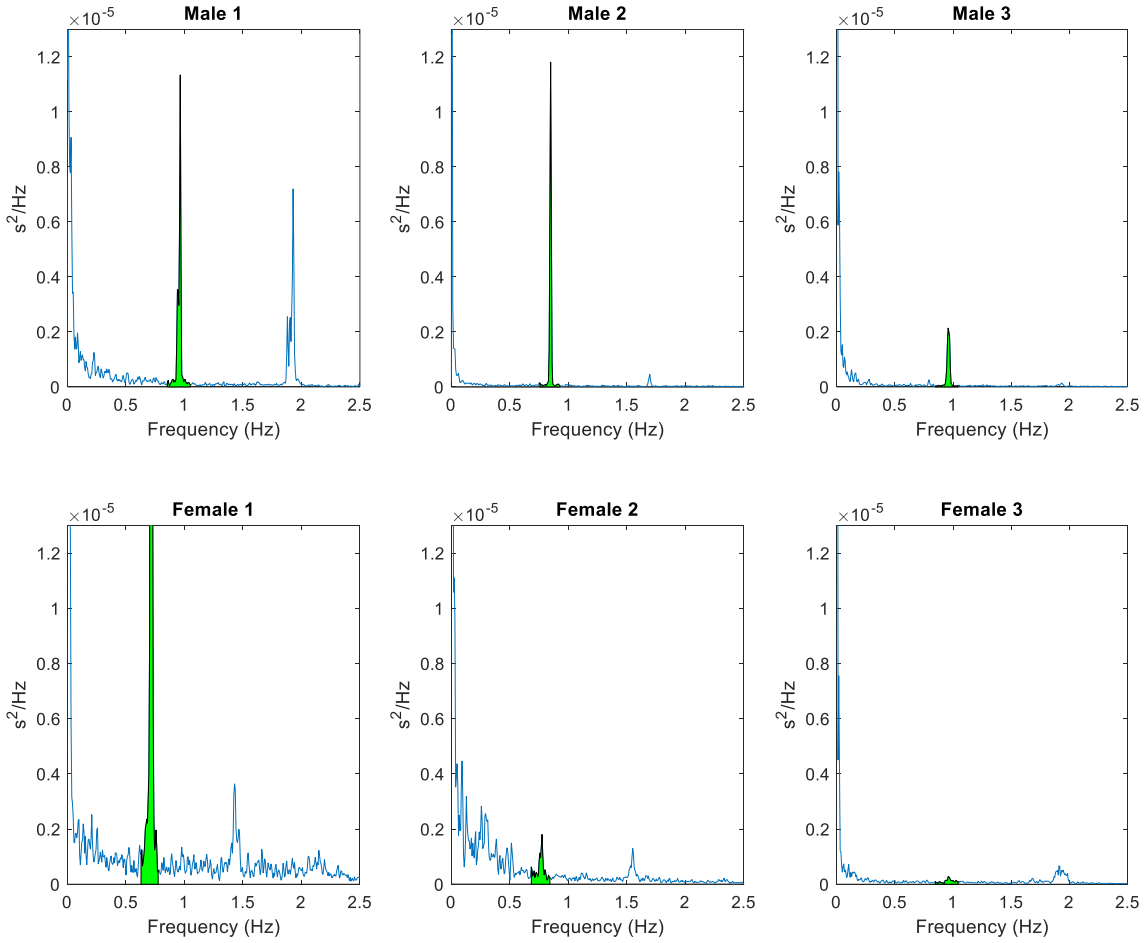

Fig. 3.6 Periodograms from 3 male and female (same animals as figure 3.1) rats recorded during a spontaneous breathing baseline analyzed with respiratory peak method.

The respiratory peak power from all baseline recordings during spontaneous breathing were compared for α = 10% (figure 3.7). Males had a 52% higher mean power than females, but there was no significant difference (p=0.35). The data sets were then filtered to only gaussian data (figure 3.8). In the gaussian data, the males' mean respiratory peak power was significantly (p=0.02) higher (447%) than the females.

Table 3.4 Animal Stability Parameters and Respiratory Band Powers for Figure 6

Animal	**Mean HR** (Hz)	**Mean BP** (mmHg)	**Respiration** (Hz)	**Power** $\alpha = 10\%$ (s^2)	**Power** $\alpha = 5\%$ (s^2)
Male 1	5.44	99.7	0.96	2.33E-07	2.18E-07
Male 2	5.61	98.9	0.85	1.68E-07	1.62E-07
Male 3	6.03	100.0	0.95	6.45E-08	6.09E-08
Female 1	4.91	96.0	0.71	1.27E-06	1.18E-06
Female 2	5.60	101.6	0.77	8.75E-08	6.36E-08
Female 3	5.50	99.0	0.95	2.12E-08	1.29E-08

To see the effects of different respiratory peak integration widths (the α value) integrated on the power spectrum, measurements were repeated for $\alpha = 5\%$ (figures 3.9, 3.10). In the data set with all the animals, the means and variances were very similar to the values from $\alpha = 10\%$, and there was no significant difference between males and females (p=0.28). When the data was restricted to gaussian only, the males' mean respiratory band power was significantly (p=0.01) higher (496%) than the females. For $\alpha = 10\%$ and 5%, the gaussian data had a smaller relative variance, greater significance (smaller p value), and smaller coefficient of variation (table 3.5).

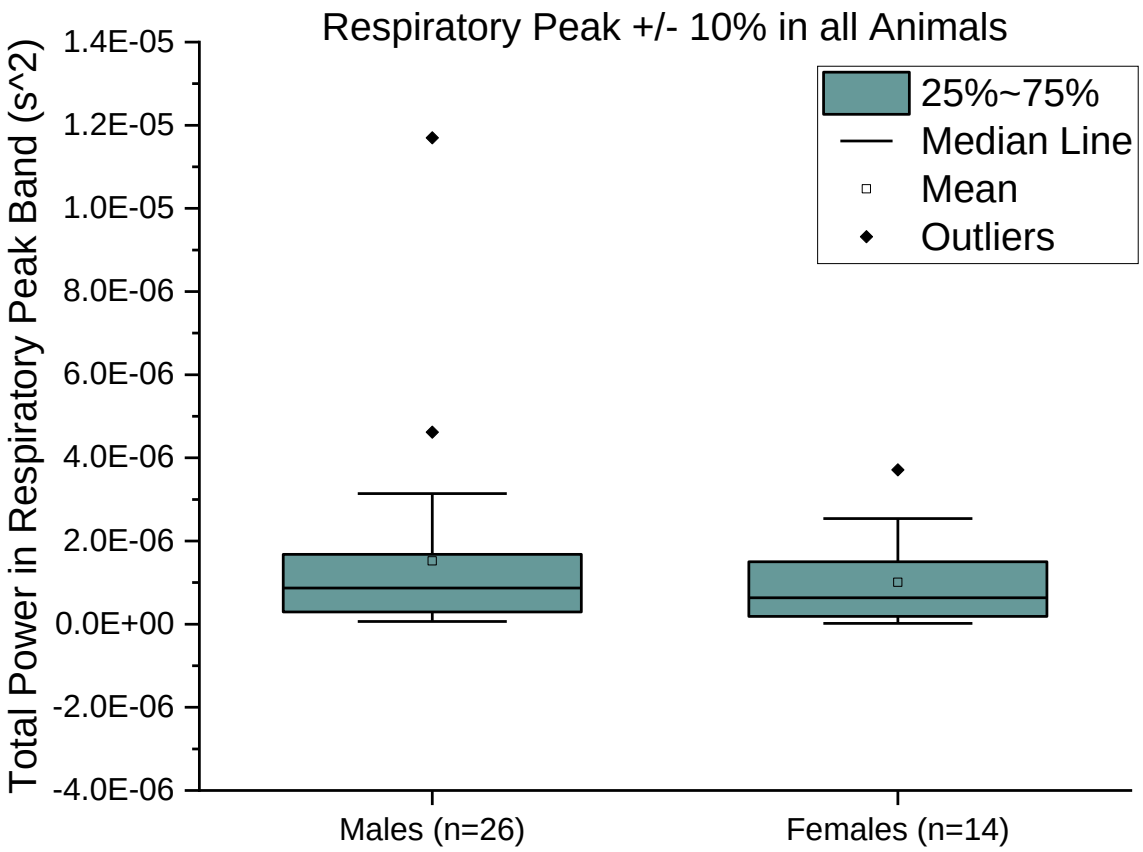

Fig. 3.7 Respiratory band total power for 10 minutes of ECG data during spontaneous breathing baseline. Animals are not discriminated based on ECG histogram distribution type. Mean respiratory band power was higher in males (n=26) than females (n=14). Integrated total powers (mean +/- SD, units are s^2): Male respiratory band power = 1.52 +/- 2.36 E-06. Female respiratory band power = 1.00 +/- 1.08 E-06.

After analyzing baselines taken during spontaneous breathing, baselines were analyzed from respirator-controlled breathing. The fixed respiration rate of 62 bpm expectedly (because of RSA) caused a large sharp respiration peak to occur at 1.03 (62/60) Hz on the power spectrum in most animals (figure 3.11). Some animals failed to adjust to the respirator, causing multiple respiration peaks and/or other crisis activity to be seen (figure 3.12), and were not considered for analysis.

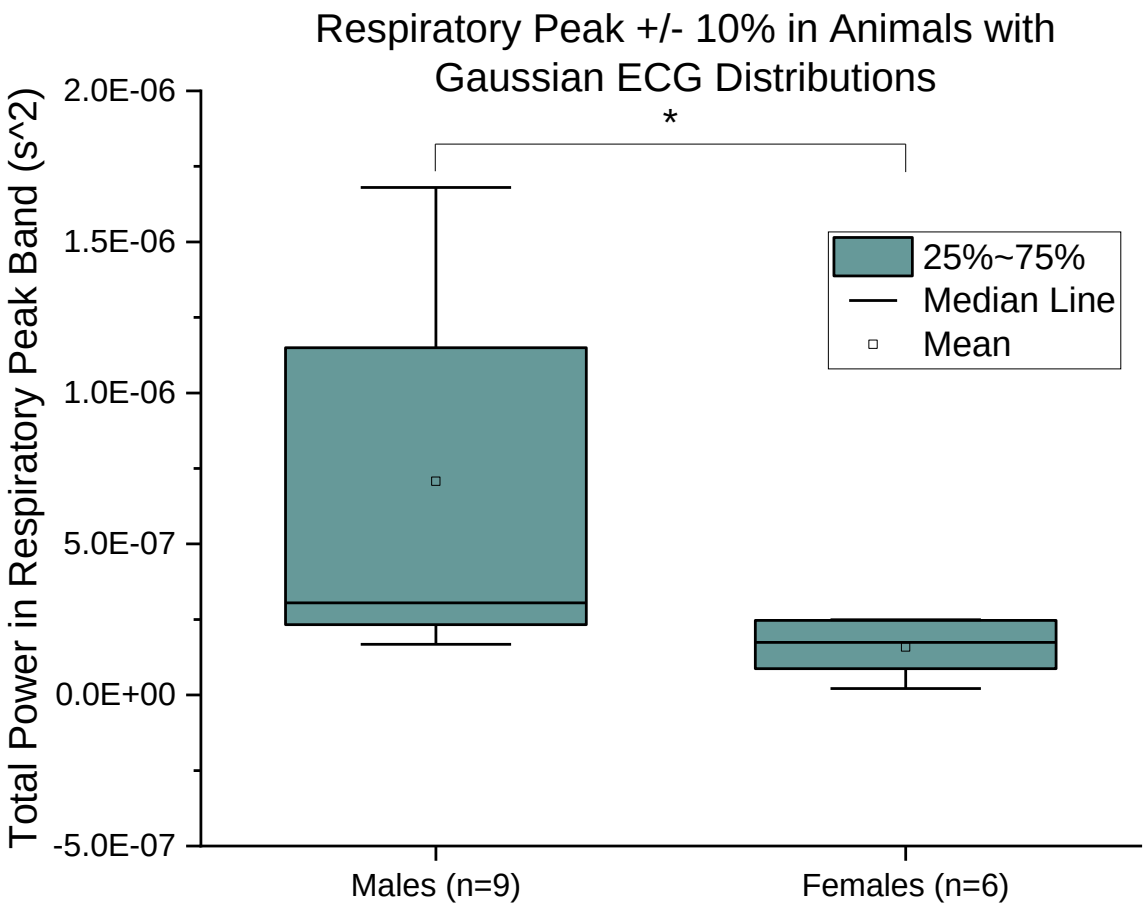

Fig. 3.8 Respiratory band total power for 10 minutes of ECG data during spontaneous breathing baseline. Only animals with an apparent gaussian ECG histogram distribution are included. Mean respiratory band power was higher in males (n=9) than females (n=6). Integrated total powers (mean +/- SD, units are s^2): Male respiratory band power = 7.07 +/- 1.98 E-07. Female respiratory band power = 15.87 +/- 9.33 E-08.

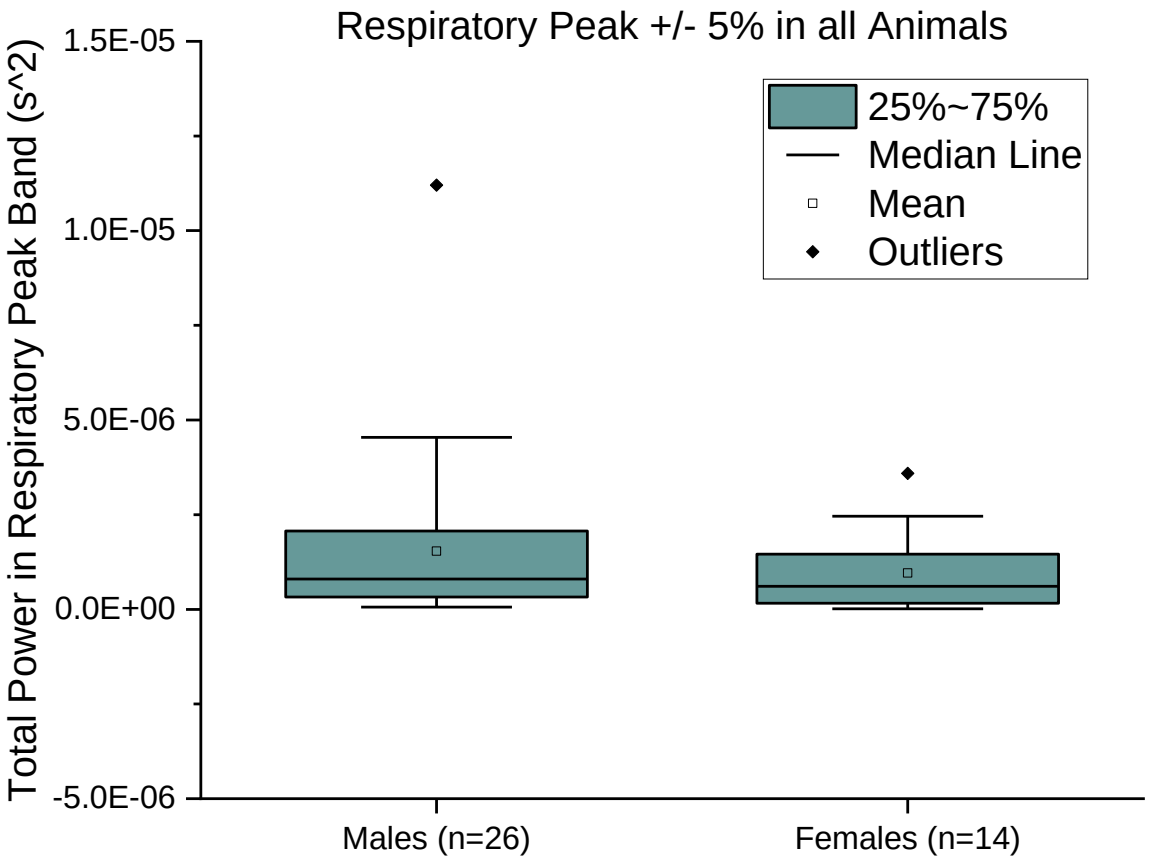

Fig. 3.9 Respiratory band total power for 10 minutes of ECG data during spontaneous breathing baseline. Animals are not discriminated based on ECG histogram distribution type. Mean respiratory band power was higher in males (n=26) than females (n=14). Integrated total powers (mean +/- SD, units are s^2): Male respiratory band power = 1.53 +/- 2.27 E-06. Female respiratory band power = 9.61 +/- 10.61 E-06.

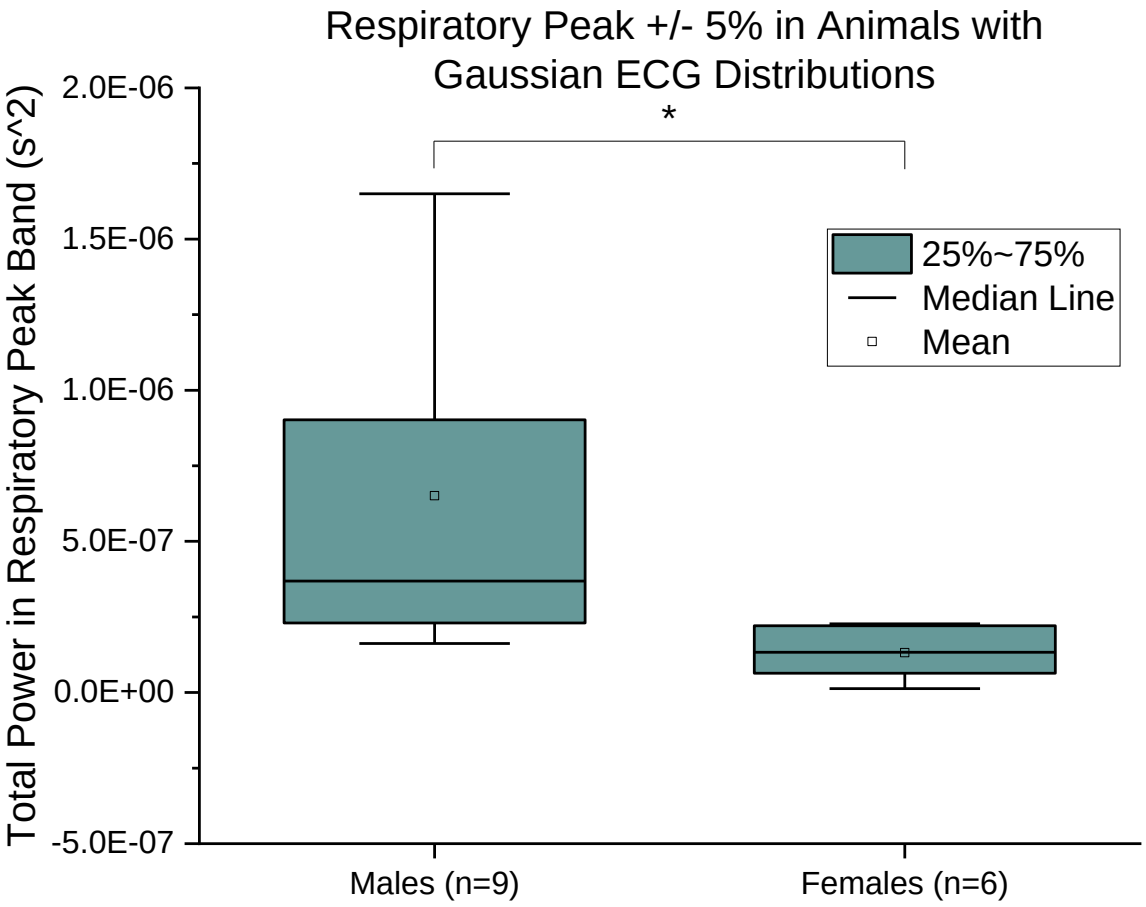

Fig. 3.10 Respiratory band total power for 10 minutes of ECG data during spontaneous breathing baseline. Only animals with an apparent gaussian ECG histogram distribution are included. Mean respiratory band power was higher in males (n=9) than females (n=6). Integrated total powers (mean +/- SD, units are s^2): Male respiratory band power = 6.50 +/- 5.24 E-07. Female respiratory band power = 13.17 +/- 8.63 E-08.

Table 3.5 Comparing Coefficients of Variation to P Values for Males and Females in Respiratory Peak Analysis

ECG Histogram Distribution	**Sex**	**Respiratory Band α Value**	**Coefficient of Variation**	**P Value**
All (figures 3.7,3.8)	Male	10	1.55	0.35
	Female	10	1.08	
All (figures 3.7,3.8)	Male	5	1.47	0.28
	Female	5	1.10	
Gaussian (figures 3.9,3.10)	Male	10	0.28	0.02
	Female	10	0.58	
Gaussian (figures 3.9,3.10)	Male	5	0.80	0.01
	Female	5	0.01	

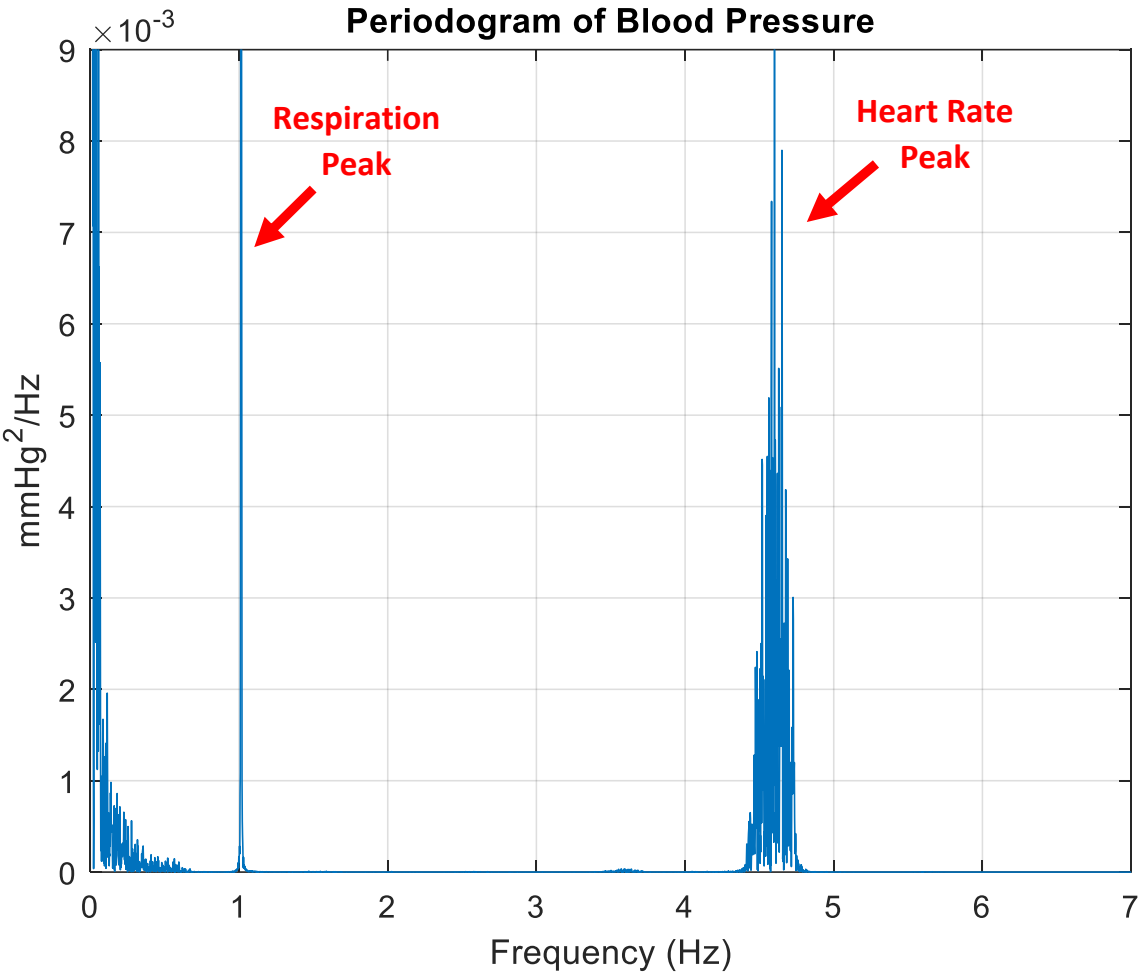

Fig. 3.11 Periodogram generated from a male rat that successfully adjusted to the respirator, indicated by the single respiration peak centered at the respirator frequency (1.03 Hz).

A total of 3 males and 3 females were used for respirator controlled breathing baseline analysis. Analysis was performed using the previous procedures of absolute power integration in the LF and HF bands (figure 3.13) and normalization (figure 3.14). In absolute measures, the variance in the males LF power was relatively low, but there was no significant difference between males and females in either the LF power (p=0.18) or HF power (p=0.62). A smaller coefficient of variation correlated to a smaller p value (table 3.6). Normalizing the data (table 3.7) revealed no significance between males and females in LF (p=0.22) or HF (p=0.22)power.

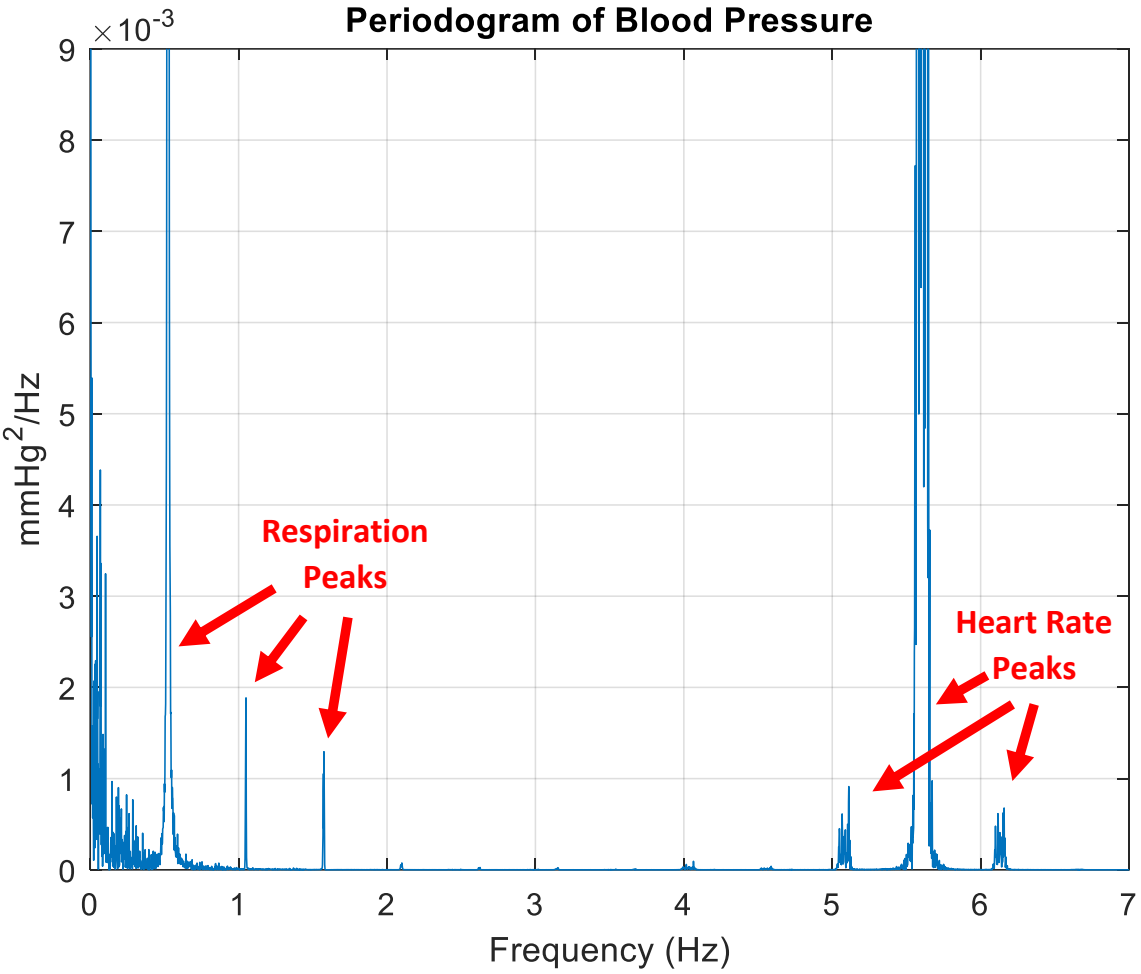

Fig. 3.12 Periodogram from a male rat that failed to adjust to the respirator, indicated by the a lack of a single respiratory peak at 1.03 Hz.

Table 3.6 Comparing Coefficients of Variation to P Values for Absolute Measurements of Frequency Bands during Respirator Controlled Breathing

Sex	**Frequency Band**	**Coefficient of Variation**	**P Value**
Male	LF	0.09	0.18
Female	LF	0.67	
Male	HF	0.75	0.62
Female	HF	0.52	

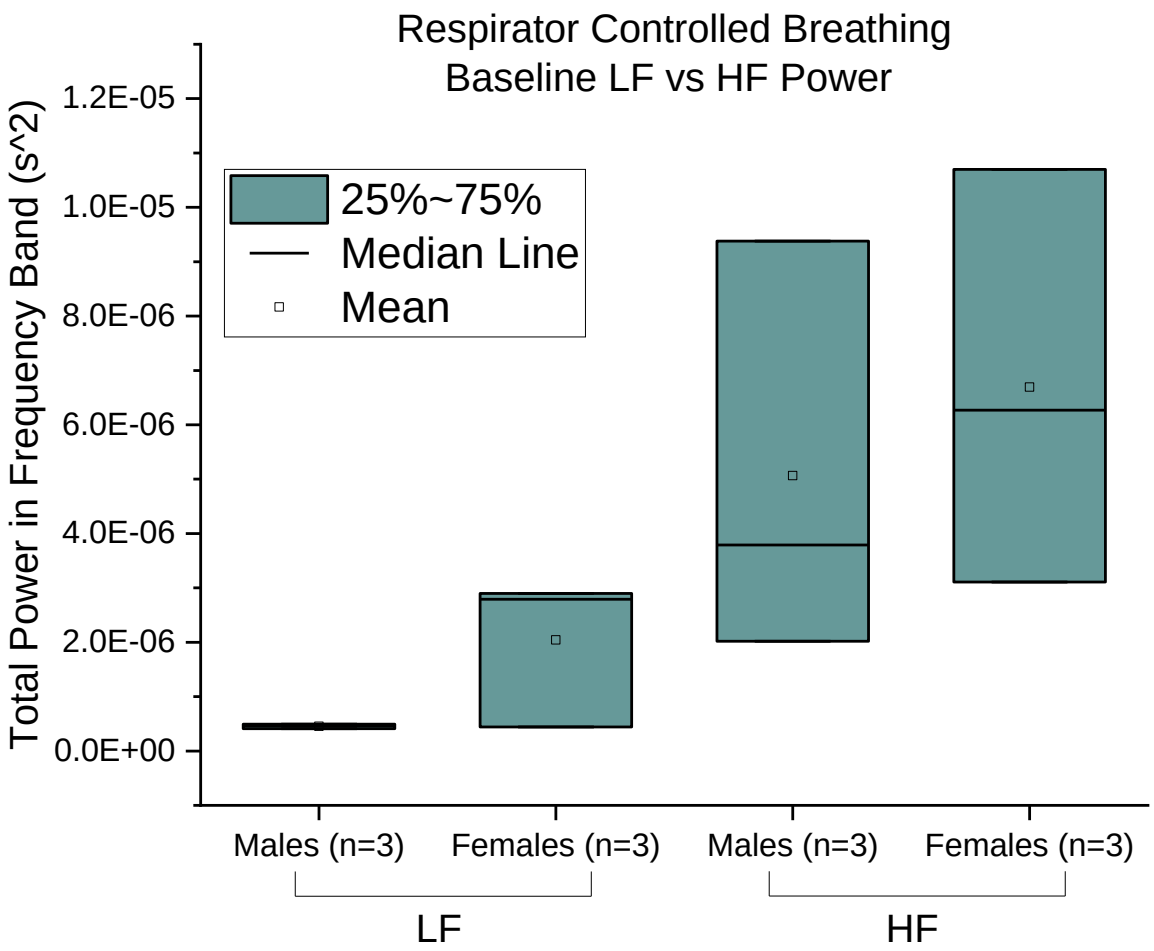

Fig. 3.13 Comparing LF and HF total power for 10 minutes of ECG data during respirator controlled breathing baseline. Two males had an apparent gaussian ECG histogram, and one had an apparent bimodal. Two females had an apparent gaussian ECG histogram, and one had an apparent bimodal. Mean LF and HF power was higher in females (n=3) than males (n=3). Integrated total powers (mean +/- SD, units are s^2): Male LF power = 4.54 +/- 0.41 E-07. Female LF power = 2.04 +/- 1.38 E-06. Male HF power = 5.06 +/- 3.84 E-06. Female HF power = 6.69 +/- 3.53 E-06.

In the respirator-controlled breathing baselines, respiratory peak analysis (figure 3.15; $\alpha = 10\%$, figure 3.16; $\alpha = 5\%$) revealed no significant difference between males and females for either $\alpha = 10\%$ (p = 0.58) or 5% (p=0.52).

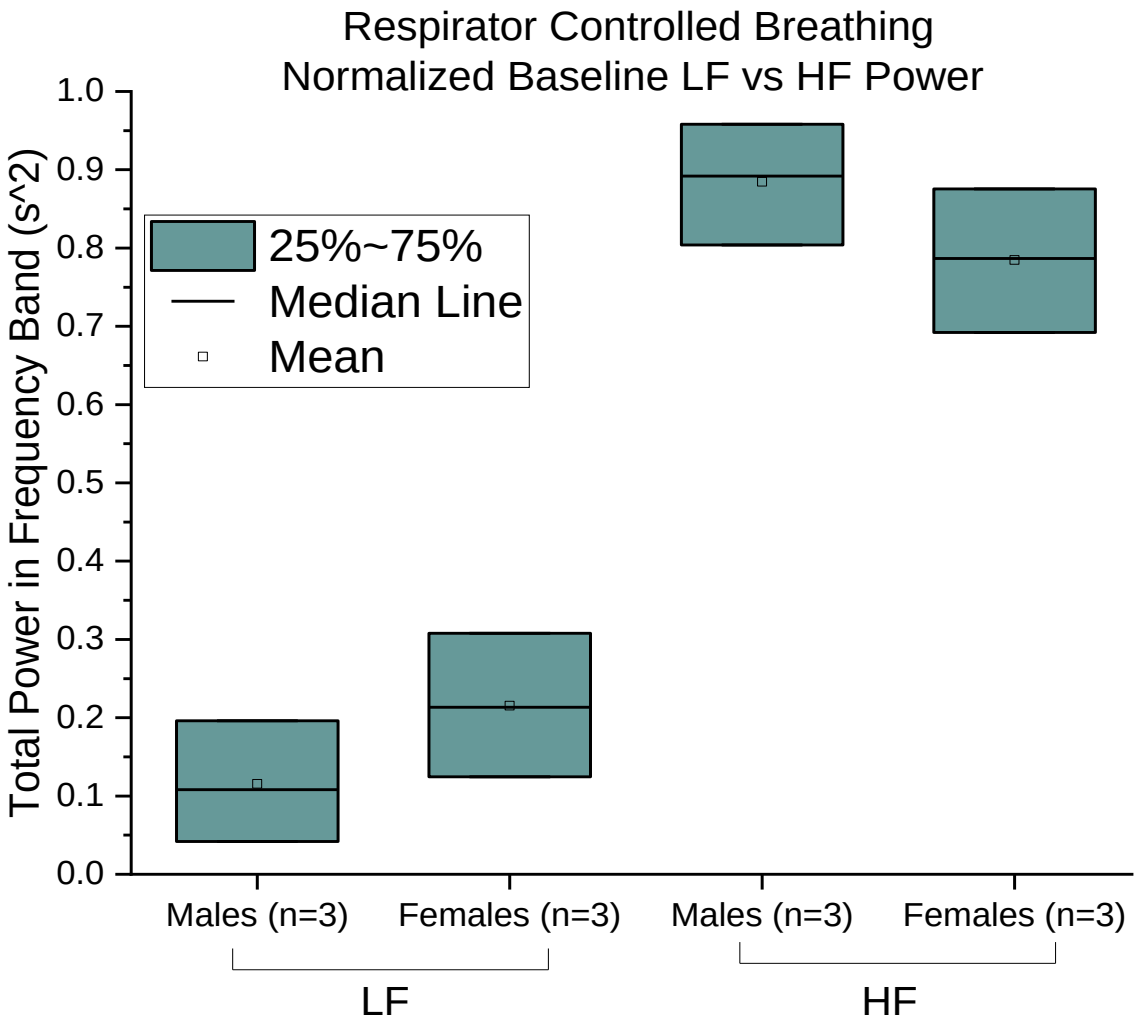

Fig. 3.14 Comparing normalized LF and HF total power for 10 minutes of ECG data during respirator controlled breathing baseline. Mean normalized LF power was higher in females (n=3) than males (n=3). Mean normalized HF power was higher in males (n=3) than females (n=3). Integrated total powers (mean +/- SD, units are s^2): Male LF power = 0.11 +/- 0.07. Female LF power 0.21 +/- 0.09. Male HF power = 0.88 +/- 0.07. Female HF power = 0.78 +/- 0.09.

Table 3.7 Comparing Coefficients of Variation to P Values for Normalized Measurements of Frequency Bands during Respirator Controlled Breathing

Sex	**Frequency Band (Normalized)**	**Coefficient of Variation**	**P Value**
Male	LF	0.63	0.22
Female	LF	0.42	
Male	HF	0.09	0.22
Female	HF	0.11	

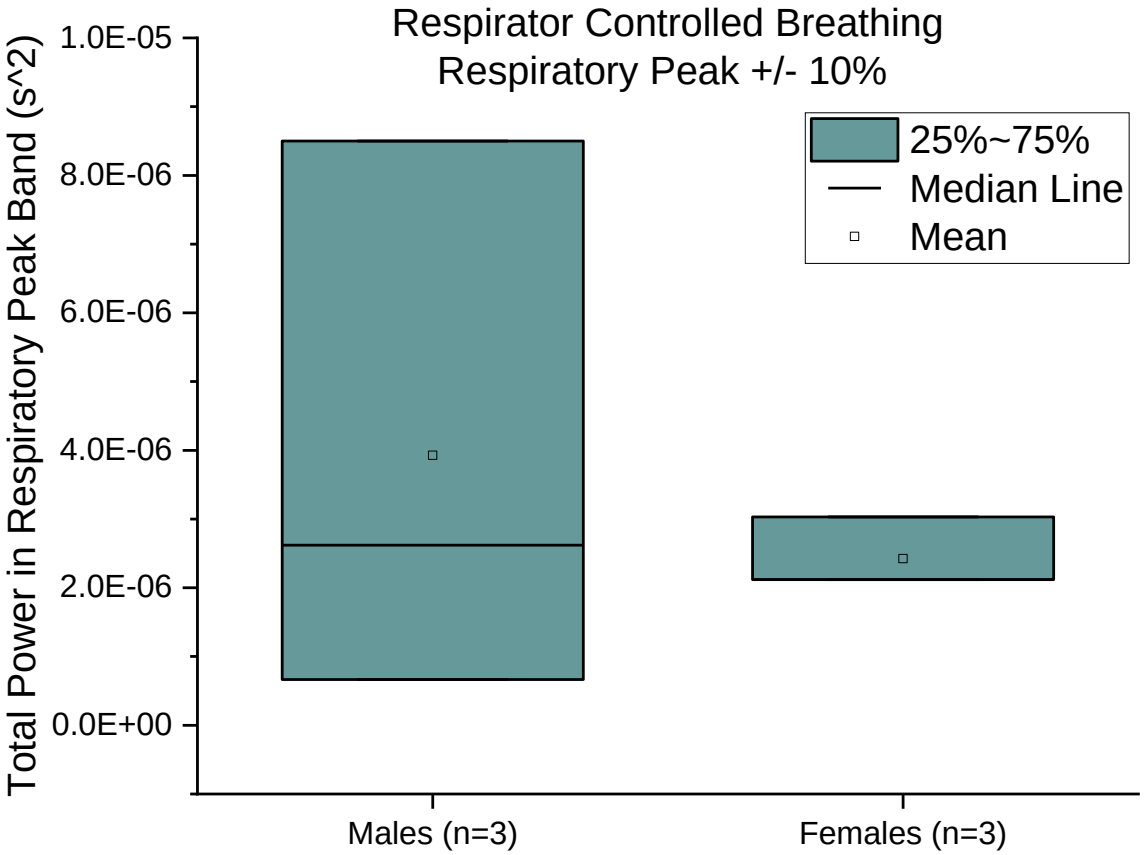

Fig. 3.15 Respiratory band total power for 10 minutes of ECG data during respirator controlled breathing baseline. Mean respiratory band power was higher in males (n=3) than females (n=3). Integrated total powers (mean +/- SD, units are s^2): Male respiratory band power = 3.92 +/- 4.07 E-06. Female respiratory band power = 2.42 +/- 0.52 E-06.

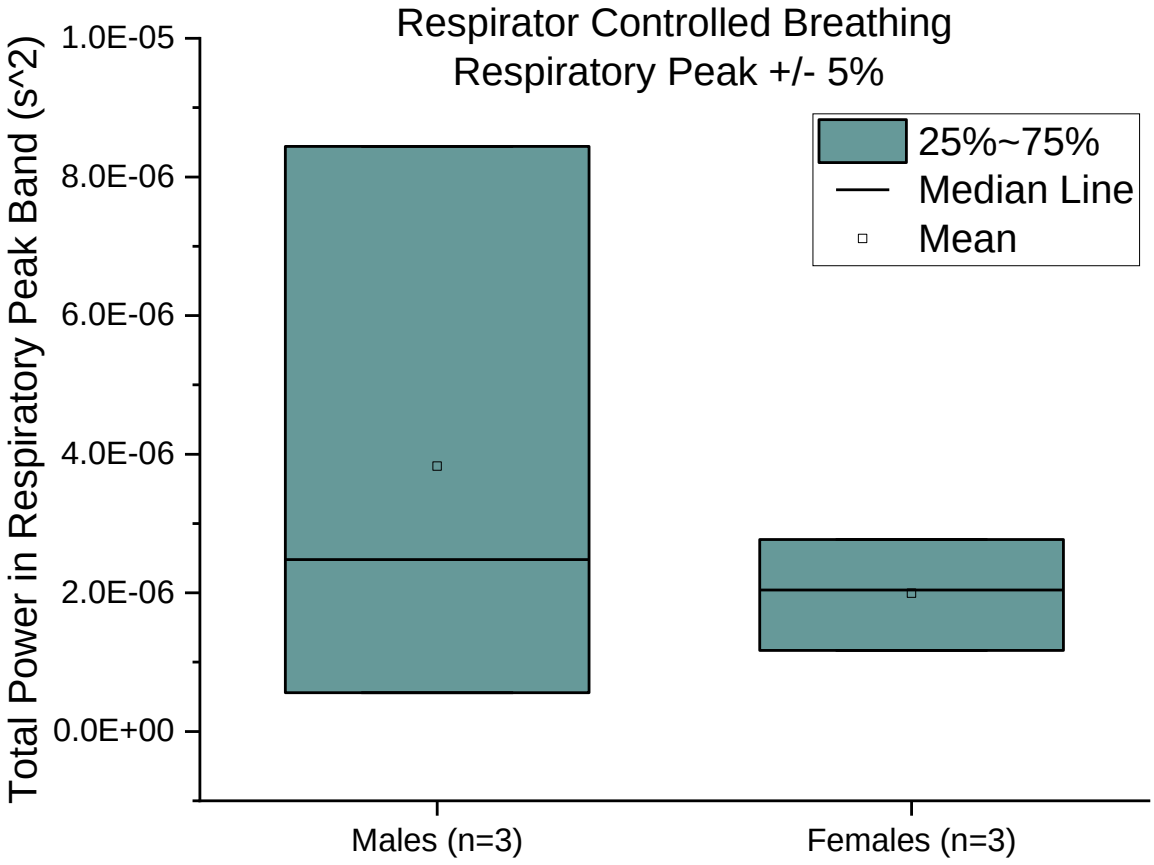

Fig. 3.16 Respiratory band total power for 10 minutes of ECG data during respirator controlled breathing baseline. Mean respiratory band power was higher in males (n=3) than females (n=3). Integrated total powers (mean +/- SD, units are s^2): Male respiratory band power = 3.82 +/- 4.10 E-06. Female respiratory band power = 1.99 +/- 0.80 E-06.

Table 3.8 Comparing Coefficients of Variation to P Values for Respiratory Bands during Respirator Controlled Breathing

Sex	**Respiratory Band α Value**	**Coefficient of Variation**	**P Value**
Male	10	1.03	0.58
Female	10	0.21	
Male	5	1.07	0.52
Female	5	0.40	

For analysis during selective activation of the BRx depressor response (chronic stimulation of the ADN), a total of 3 females (on a respirator) were used. The chronic stimulation resulted in an average decrease in HR of 0.14 +/- 0.30 Hz and average decrease in BP of 34.00 +/- 15 mmHg (figure 3.17; top, middle), consistent with a previous Schild lab study [8]. No males had successful chronic stimulation trials due to various protocol issues, such as the electrodes shorting out during the stimulation.

A respirator-controlled breathing baseline was used as a paired control for each chronic stimulation in HRV analysis (figure 3.18). Because previous frequency band analysis indicated no significance for absolute and normalized measurements, only absolute measures of HF were compared for frequency band analysis because they were marginally insignificant for gaussian data. Respiratory peak analysis was also performed for $\alpha = 10\%$ and 5%. In all measurements, there was an increase in average power, despite no significant differences observed (HF: p=0.32; $\alpha = 10\%$, p = 0.19; $\alpha = 5\%$, p = 0.28). The author would like to note that one of three data sets from the stimulation trials was possibly an outlier, as its power density spectrum was highly inconsistent compared to the other two stimulations and their paired baselines.

To further assess how HRV is affected throughout the duration of the stimulation protocol, three five minute windows were analyzed using the HRV algorithm (adjusted to analyze five minute intervals of ECG). These windows were taken at the beginning (first five minutes), middle (middle five minutes), and end (last five minutes) of the chronic stimulation (figure 3.17). There was a consistent decrease in LF and HF power throughout the course of the stimulation.

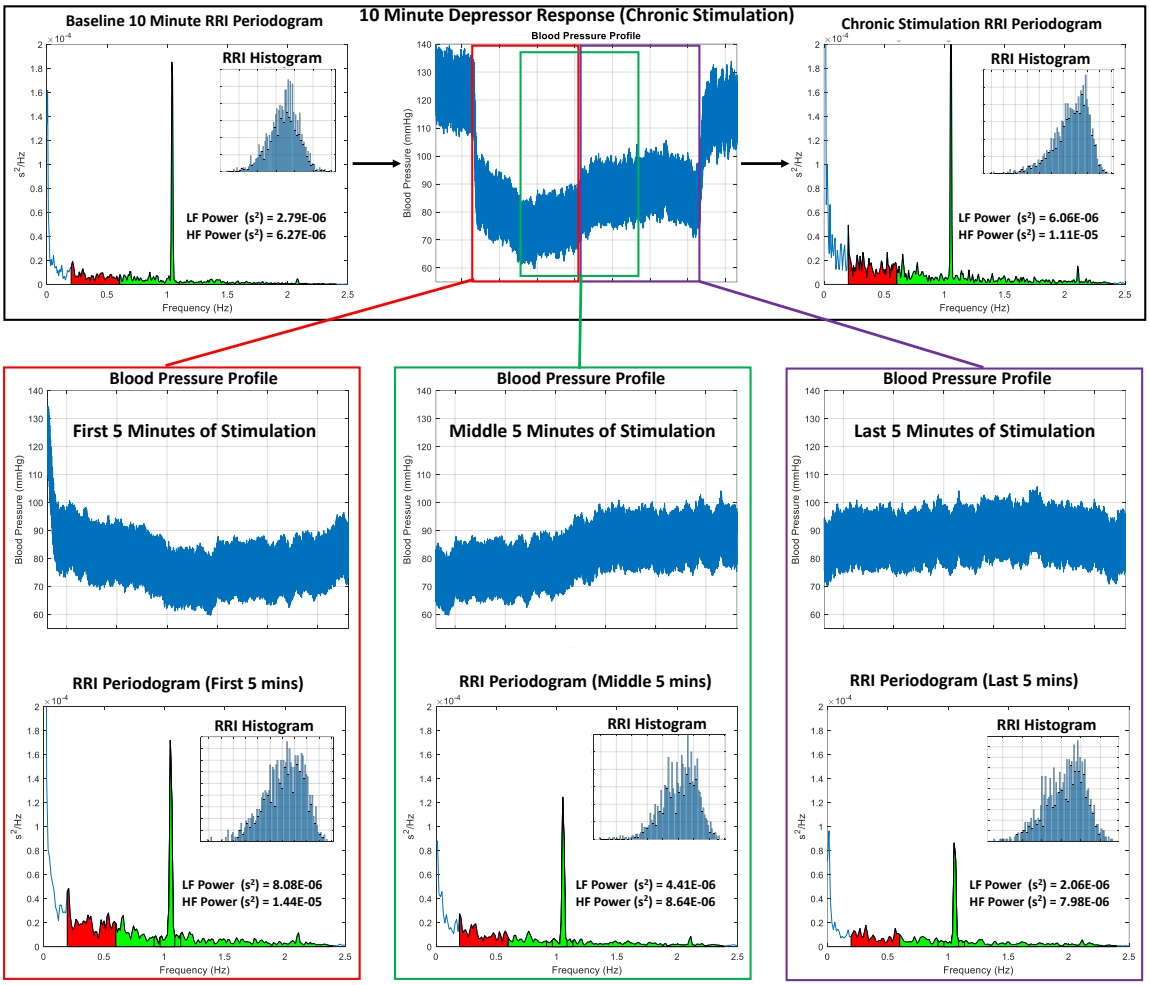

Fig. 3.17 HRV analysis and blood pressure response during chronic stimulation. Ten minute windows (top) are compared to a sliding five minute window (bottom). Starting from the beginning and moving towards the end of the stimulation, there is a consistent decrease in the power bands.

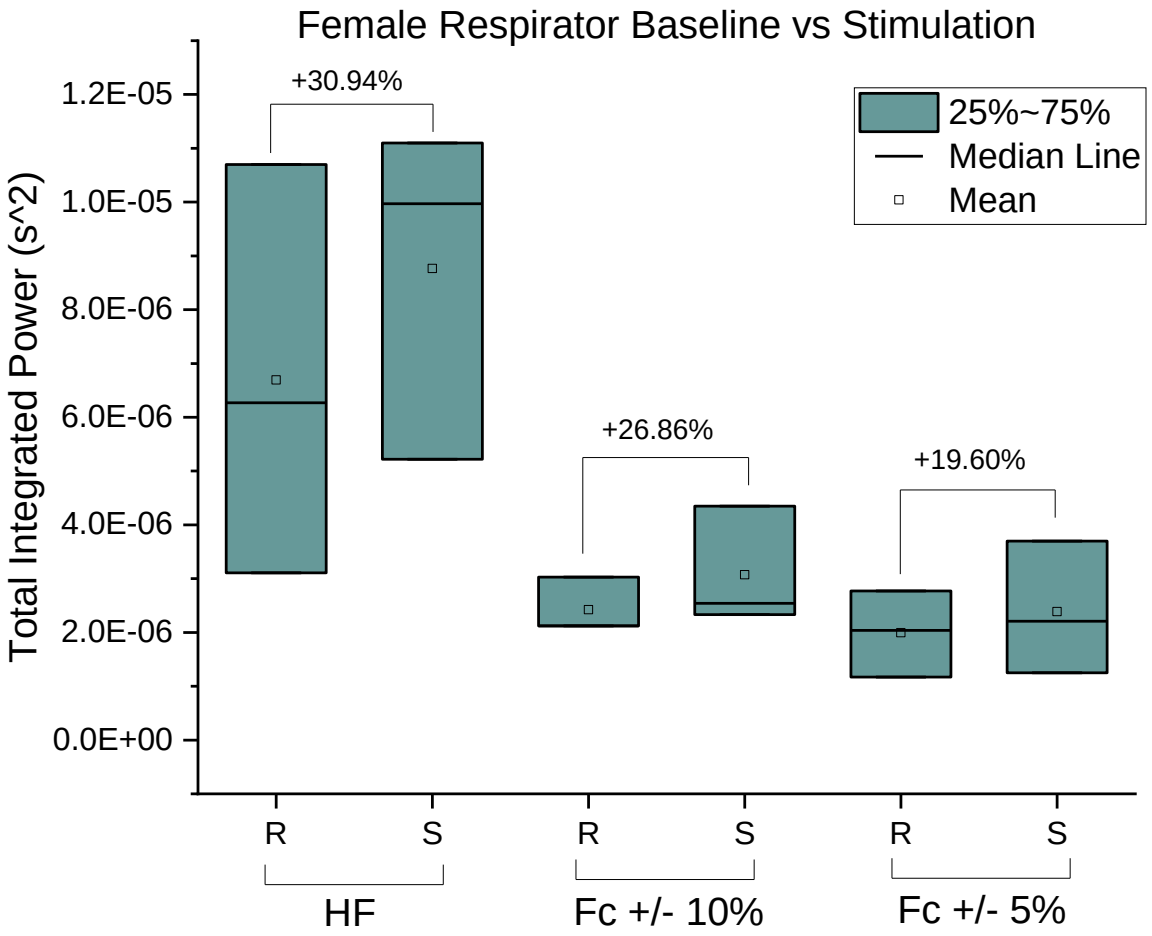

Fig. 3.18 R = Respirator Baseline. S = Stimulation. Comparing HF and respiratory band power for 10 minutes of ECG data during respirator controlled breathing baseline and its immediately followed paired stimulation. Mean power increased in all cases. Integrated total powers (mean +/- SD, units are s^2): HF R power = 6.69 +/- 3.81 E-06. HF S power = 8.76 +/- 3.12 E-06. $\alpha = 10\%$ R power = 2.42 +/- 0.52 E-06. $\alpha = 10\%$ S power = 3.07 +/- 1.11 E-06. $\alpha = 5\%$ R power = 1.99 +/- 0.80 E-06. $\alpha = 5\%$ S power = 2.38 +/- 1.23 E-06.

To test if shorter durations, including the five minute windows analyzed during stimulation, would be viable for HRV analysis, all previous tests were repeated using five-minute-long ECGs (half the duration). These five minutes portions were taken from the center of the ten-minute segments (going from 2.5 minutes to 7.5 minutes in any ten-minute ECG's recording). In all measurements with five minutes of data, the only significant differences were those with significant differences from ten-minute ECG HRV analysis (respiratory peak analysis for animals with gaussian ECGs, for $\alpha = 10\%$ and 5%). However, significance did increase for the five-minute recording for both α values (table 3.9). It is worth noting that the five-minute measurement comparing absolute HF measures between gaussian males and females had a p value of 0.05001 (still marginally insignificant).

Table 3.9 Comparing P values for Respiratory Peak analysis for Ten and Five Minutes of ECG Data

Duration of ECG (Minutes)	α **= 10% P Value**	α **= 5% P Value**
10	0.024	0.018
5	0.019	0.017

3.5 Aim 2: Exploring Correlations between Baroreflex Sensitivity and Heart Rate Variability Analysis

BRS analysis was performed on the three females with paired respirator-controlled breathing baselines and stimulations using the slope method. An ascending (two increasing RRI and BP values) and descending (two decreasing RRI and BP values) BRS value was calculated for the baseline recording immediately before the paired stimulation, as well as nine minutes into the stimulation to mitigate transient effects. There was no significant difference (p=0.45) between the paired baseline and stimulation ascending BRS values (figure 3.19). There was also no significant difference (p=0.17) between the paired baseline and stimulation descending BRS values (figure 3.20).

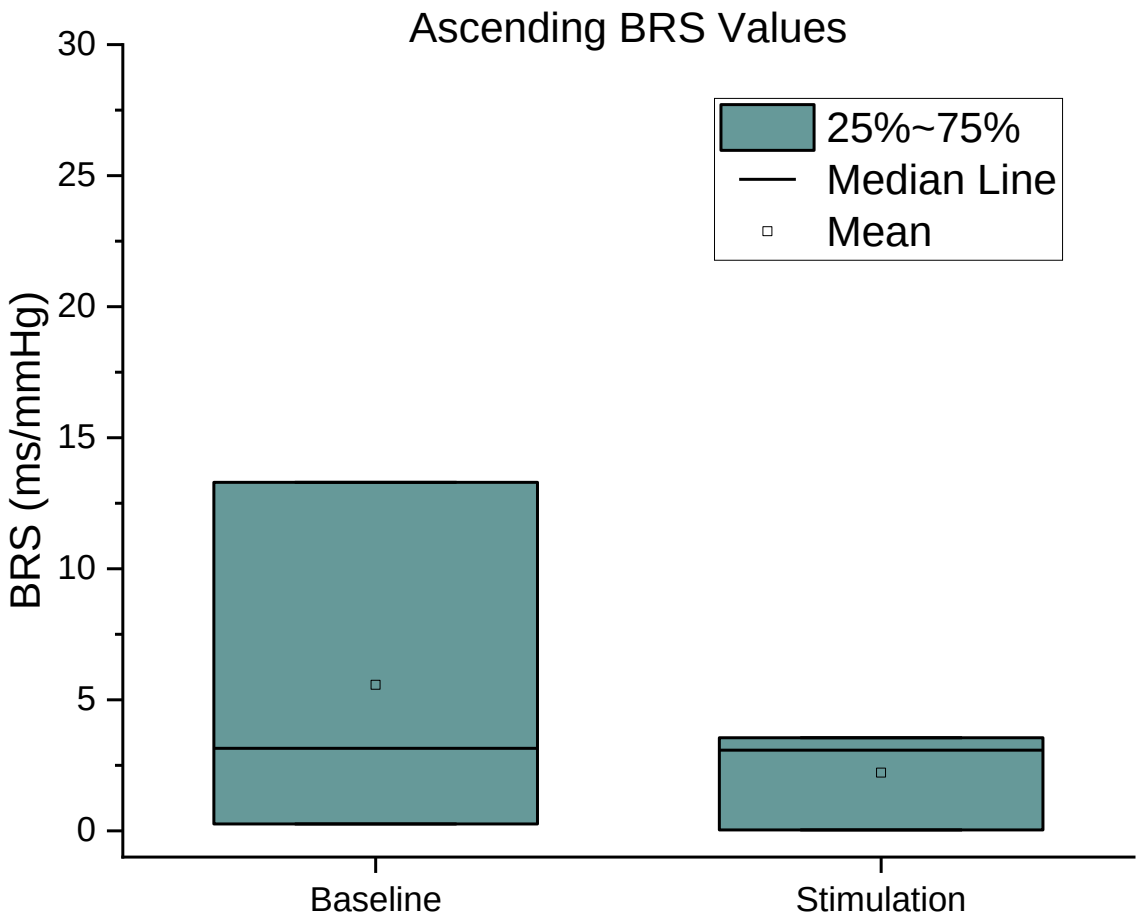

Fig. 3.19 Ascending BRS values during baseline and stimulation for female rats.

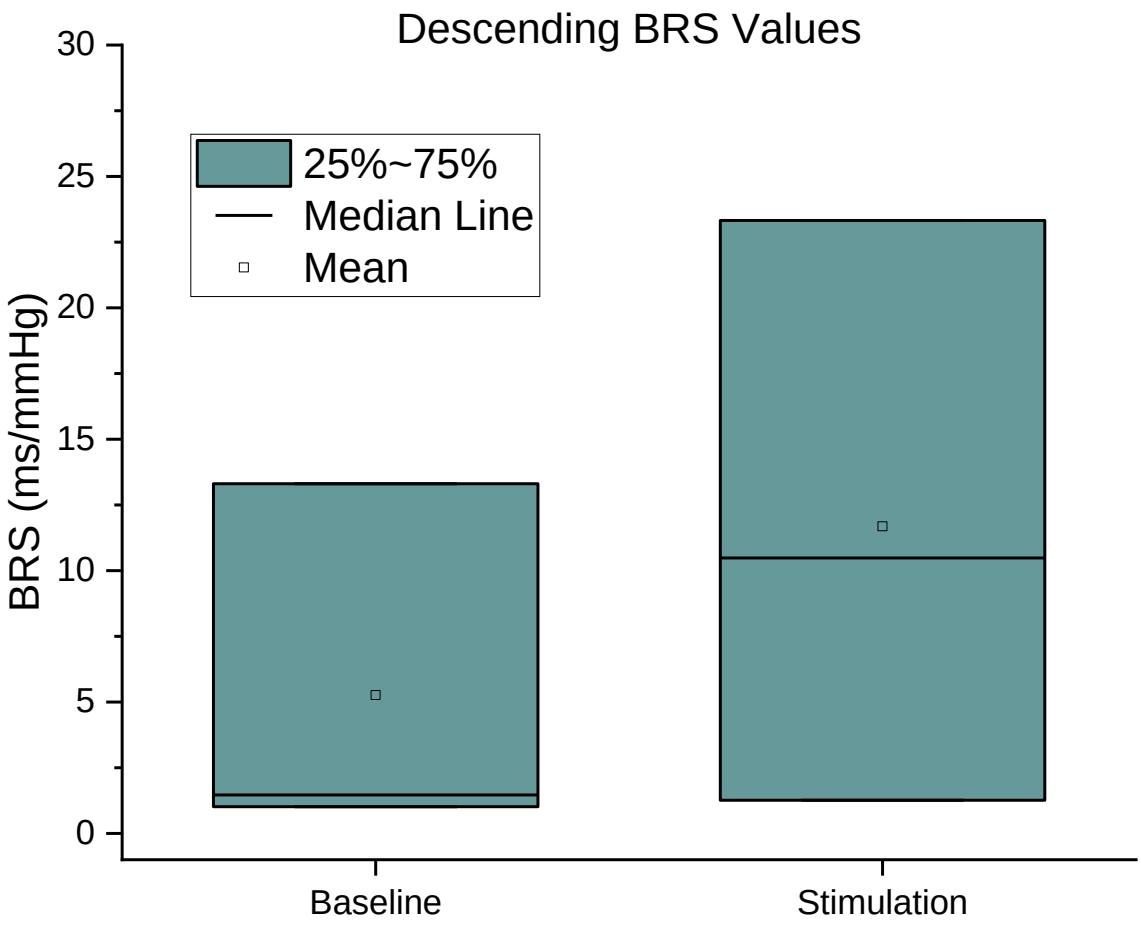

Fig. 3.20 Descending BRS values during baseline and stimulation for female rats.

The BRS values were compared to the significant HRV measurements (respiratory band power) from ten-minute respirator controlled breathing baseline (table 3.10) and stimulation (table 3.11) recordings. These measurements were repeated for five-minute recordings (tables 3.12, 3.13). There was no consistent correlation between BRS values and the respiratory band power in any of the measurements for both ten and five minutes. The author would like to note that female 3 (tables 3.10-3.13) is a possible outlier.

Table 3.10 Comparing Baseline BRS Values to Respiratory Peak Analysis for 10 Minute ECG Recordings

Animal	**Ascending BRS (ms/mmHg)**	**Descending BRS (ms/mmHg)**	**Respiratory Band Power $\alpha = 10\%$ (s^2)**	**Respiratory Band Power $\alpha = 5\%$ (s^2)**
Female 1	3.15	1.46	2.12E-06	2.04E-06
Female 2	0.26	1.01	3.03E-06	2.77E-06
Female 3	13.29	13.30	2.12E-06	1.17E-06

Table 3.11 Comparing Stimulation BRS Values to Respiratory Peak Analysis for 10 Minute ECG Recordings

Animal	**Ascending BRS (ms/mmHg)**	**Descending BRS (ms/mmHg)**	**Respiratory Band Power $\alpha = 10\%$ (s^2)**	**Respiratory Band Power $\alpha = 5\%$ (s^2)**
Female 1	0.19	10.47	2.12E-06	2.04E-06
Female 2	3.07	1.25	3.03E-06	2.77E-06
Female 3	3.54	23.32	2.12E-06	1.17E-06

Table 3.12 Comparing Baseline BRS Values to Respiratory Peak Analysis for 5 Minute ECG Recordings

Animal	**Ascending BRS (ms/mmHg)**	**Descending BRS (ms/mmHg)**	**Respiratory Band Power $\alpha = 10\%$ (s^2)**	**Respiratory Band Power $\alpha = 5\%$ (s^2)**
Female 1	3.15	1.46	2.16E-06	2.07E-06
Female 2	0.26	1.01	3.33E-06	3.05E-06
Female 3	13.29	13.30	2.06E-06	1.09E-06

Table 3.13 Comparing Stimulation BRS Values to Respiratory Peak Analysis for 5 Minute ECG Recordings

Animal	**Ascending BRS (ms/mmHg)**	**Descending BRS (ms/mmHg)**	**Respiratory Band Power $\alpha = 10\%$ (s^2)**	**Respiratory Band Power $\alpha = 5\%$ (s^2)**
Female 1	0.19	10.47	2.61E-06	2.33E-06
Female 2	3.07	1.25	3.68E-06	3.24E-06
Female 3	3.54	23.32	1.85E-06	9.78E-07

CHAPTER 4. DISCUSSION

4.1 General Conclusions

This thesis investigated HRV techniques for quantifying autonomic tone. The FFT and PSD frequency transform method was utilized because of its experimentally fitting assumptions and persistent use in research. This work demonstrated that there are strong correlations between the power spectrum of HRV and the ANS, particularly with the appearance of the respiratory peak in the power spectrum. The most prominent findings included: (1) there are many caveats involving cardiovascular stability that affect HRV, which results in a large amount of variance in the control system and associated power spectrums; (2) frequency band analysis, with and without applied normalization, is not consistently adequate for precisely measuring a sexual dimorphism in HRV; (3) respiratory peak analysis is a precise measurement that demonstrated sexual dimorphism in HRV; (4) there is a consistent increase in HRV during sustained electrical activation of the BRx depressor response; and (5) the slope method for BRS is likely not adequate for quantifying the BRx during sustained electrical activation of the BRx depressor response.

4.2 Assessing Cardiovascular Stability

Many of the measurements in this work involved considering more stability parameters beyond just HR, BP, and respiration, with additional discrimination based the ECG histogram distribution type (e.g. figure 3.2 versus figure 3.3) It is important to note that this method does not simply remove outliers to demonstrate significance.

Rather, this more strongly justifies the assumption of stationarity, which implies strong cardiovascular stability. Furthermore, it removes a serious bias in the data because non-gaussian ECG histogram distributions have more variability around the mean than gaussian ones. Because HRV quantifies the variability around the mean heart rate, a non-gaussian ECG histogram has higher magnitudes of power in the power spectrum. This practice of more carefully considering viable data has been extensively utilized in recent HRV studies [24,41], whereby data sets for HRV in humans is filtered down from tens of thousands of potential participants to hundreds based on several parameters relating to cardiovascular health (medical history, drug use, lifestyle, etc.). However, even with this additional criteria, there was still substantial variance in the data, especially in the frequency band analysis. In the following sections, the data that is additionally filtered based on having an apparent gaussian ECG histogram will be referred to as 'gaussian' data.

4.3 Methods for Quantifying the Power Spectrum

4.3.1 Analysis Method 1: Quantifying Absolute Measures of LF and HF bands.

The first frequency band technique compared integrating the absolute power contained in the LF and HF bands in the power spectrum between males and females. Even with animals that had very similar stability profiles (table 3.1), the observed power spectrums were often very different in overall power and specific frequency peaks (figure 3.1). Because of this variance, it was not surprising that there was no significant difference in the LF bands between males and females (figure 3.2). To quantify this variance with respect to the mean power, the coefficients of variation for the LF bands were calculated (table 3.2). The coefficients of variation were greater than one, indicating a variance greater than the mean. This large amount of variance was observed in the HF band power too (figure 3.2; table 3.2), where males had 63% higher average HF power than females, but there was no significant difference

again. When the data sets were restricted to gaussian only data and compared, there was still no significant difference in either the LF or HF frequency band (figure 3.3). However, the HF band measurement with only gaussian data had a p value of 0.052, down from 0.17, demonstrating the necessity in restricting the data to prevent a bias based on the ECG histogram distribution.

Based on these findings of absolute measures in the frequency bands, the LF band's absolute power measurement is not precise enough to establish any difference between males and females. This was not surprising, based on the continually growing uncertainty of what the LF band truly represents, beyond just sympathetic tone. While the HF band also didn't demonstrate any significant differences, even with the added gaussian restriction, there is a strong possibility that with more ns, the gaussian data would be significantly different between the sexes, based on the marginally insignificant p value.

4.3.2 Analysis Method 2: Quantifying Normalized Measures of LF and HF bands.

Since the absolute measures of the frequency bands had no significance, it was determined that normalizing the data was worth performing, given the large variability in the data. After normalizing the data (figures 3.4, 3.5) and repeating the frequency band measures, there was still no significance, and the p value in the gaussian data even increased (table 3.3). This was surprising, as this normalization technique is often utilized in human HRV studies and often demonstrates significant differences between males and females in the power spectrum [7, 12, 17, 21, 34, 41, 47, 51]. It may require significantly more data for the normalization technique to be adequate. It is important to note that the normalization method biases the coefficient of variation towards having a lower value, so it is not surprising that the p values were higher despite a lower coefficient of variation as compared to the absolute measures of the frequency bands.

4.3.3 Analysis Method 3: Performing Respiratory Peak Analysis for $\alpha = 10\%$ and 5%

It was hypothesized that respiratory peak analysis would be a more robust measure of HRV than frequency band analysis because of its strong connection to the PNS, whereby respiration is heavily modulated by activity in the vagal nerve. The α values of 10% and 5% were chosen based on literature [42] and so at least two values were available for comparison. Without restricting to only gaussian data (figures 3.7, 3.9), there was no significance observed for either α value (table 3.5). However, the gaussian data (figures 3.8, 3.10) was statistically significant for both values of α (table 3.5) with $p = 0.02$ for $\alpha = 10\%$ and $p = 0.01$ for $\alpha = 5\%$. This significance was expectedly correlated to lower coefficients of variation (table 3.5). The lower α values had lower p values, which is consistent with literature [42, 60]. Furthermore, this significance implies that females have lower mean respiratory band power. This was surprising because it well known that females have an overall more active parasympathetic nervous system compared to males. Therefore, it was expected that the females' respiratory band would contain more power than males. One possible explanation for this is that the female's more active PNS causes them to have more control, and thus less error in the control system. The power spectrum ultimately quantifies the variability in the time series of the RRI, so having a lower power indicates less variations in the heart rate. By having a higher control over their PNS, females may exhibit less HRV, and therefore have an associated smaller respiratory peak band. The author is unaware of any studies that support this hypothesis, and it would require more testing to demonstrate its veracity.

4.3.4 Analysis Method 4: Quantifying Frequency and Respiratory Band Measures with Respirator-Controlled Breathing

When it was demonstrated that respiration had a significant effect on the power spectrum, the author started to control for respiration with a respirator. This ad-

justment came late in the experiments, and only six animals, three males and three females, successfully adjusted to the respirator and could be used for analysis. Frequency band analysis (absolute and normalized measures) as well as respiratory peak analysis was performed on these six animals.

It was hypothesized that by controlling respiration, there would be more consistency in the respiratory peak bands in the power spectrums. However, the opposite occurred, where the data was even more variable in the absolute (figure 3.13; table 3.6) and normalized (figure 3.14; table 3.7) frequency band measurements. In the normalized data, similar trends as before were observed, where the data became even less significant.

In respiratory peak analysis, there was also no significance for both $\alpha = 10\%$ (figure 3.15) and 5% (figure 3.16). However, females had a much lower coefficient of variation than males (table 3.8), again suggesting that females have less HRV associated with respiratory modulation. The author wishes to note that the low number of ns is likely a contributor for the lack of significance, as the means were similar to those from the spontaneous breathing baseline, which were highly significant measures in respiratory peak analysis.

4.3.5 Analysis Method 5: Quantifying Frequency and Respiratory Band Measures during Focal Parasympathetic Drive of the Baroreflex

By stimulating the ADN, there is selective activation of the BRx, which causes significantly elevated activity in the PNS [8]. It was hypothesized that stimulation of the ADN would cause increases in the power of HF band and respiratory peak power. Three females were used in analysis, where each had a paired respirator baseline and stimulation. The HF band (absolute measurement) and respiratory band ($\alpha = 10\%$ and 5%) were compared for each paired baseline and stimulation (figure 3.18). There was an increase in mean power between the baseline and stimulation, but there were no significant differences in any measurement. Furthermore, the decreases in HR and

BP were consistent with a previous Schild lab study [8]. These trends suggest that more ns could demonstrate a significant difference. It would be surprising if HRV could not measure any differences in autonomic tone during stimulation.

Five minute windows (figure 3.17) were analyzed throughout the duration of the stimulation. There was an observed decrease in the LF and HF power moving from the the first window to the second and third windows, respectively. This was an interesting trend because it is expected that there will be more compensatory activity during the first five minutes of stimulation when transient effects have a great effect, relative to the end of the stimulation when the stimulated system is closer to or in steady state. This experimentally fitting observation further suggests that HRV analysis is sensitive enough to assess the transient effects of focal parasympathetic drive, and that perhaps shortening the duration of the algorithm to assess five minute intervals is appropriate (which would also be experimentally easier).

4.4 Shortening the Duration of the Data

By using ten-minutes of ECG data in all of the previous measurements, there is a strong justification that the animals had reached sufficient cardiovascular stability and satisfied the assumption of stationarity. However, it would be more useful to implement HRV in the clinical setting if shorter ECGs were acceptable. To assess the validity of shorter durations, all analyses were repeated with only five minutes of ECG data, taken from the middle of the ten minute samples. In these measurements, it was found that only the already significant measurements (respiratory peak analysis for gaussian data) were significant. However, the p value did decrease with the five minutes of data (table 3.9), suggesting that using five minutes or less of data is sufficient for HRV in a rat, which widens the possibility of collecting data, as it easier to establish shorter time spans of stability.

4.5 Comparing Baroreflex Sensitivity to Heart Rate Variability Analysis during Chronic Stimulation

The slope method of BRS was utilized because it is most commonly used in the clinical setting after perturbing the ANS [19]. It was hypothesized that the ascending and descending BRS values would correlate to the magnitude of the HRV power spectrum. However, no correlation was observed and there was no significant difference between baseline and stimulation for either ascending or descending BRS values (figures 3.19, 3.20). There was no consistency between the magnitude of the BRS value and the respiratory band measures taken from ten minutes (tables 3.10, 3.11) or five minutes (tables 3.12, 3.13) of data. The author believes this is due to the low number of ns, as well as a potential outlier in the data set. It would be surprising if BRS could not measure any differences in autonomic tone during stimulation because of the already known significant correlation between the BRx and the ANS.

4.6 Future Considerations

Based on the observations of this work, there are seemingly at least three important expansions in the data analysis to make:

1. Performing respiratory peak analysis for more values of α - studies have indicated that lower values of α demonstrate increasing levels of significance, although those studies are as restrictive in their use of data [42, 60]. This trend of significance persisted in this thesis, but utilizing smaller values than 5% for α may cause some respiratory peaks to not be fully included in the measurement, so a balance of optimization for how far α could be decreased while being physiologically justified would have to be considered.

2. Using shorter than five-minute segments of ECG - HRV analysis is often done with less than five minutes of data, and because there was strong significance in five minutes of data for respiratory peak analysis, there is the possibility of

continually decreasing the duration used while still being meaningful. While this becomes more clinically practical, great caution would have to be given to the consideration of stationarity. It would be easy to be deceived into thinking an animal is stable based on a couple minutes of ECG and BP data. Therefore, there is potential for quantifying what is the acceptable minimum duration of data that should be used in the FFT and PSD method.

3. Using more extensive BRS techniques to quantify a correlation between HRV and BRS - there are now dozens of techniques for quantifying BRS, which like HRV, have many caveats. BRS analysis can become very sophisticated, although each technique can be justified in the context of the experiment, like HRV. It is known that there is a correlation in the physiology between BRx activation and HRV, so there is likely a better method for assessing BRS than the slope method utilized in this work.

Furthermore, it would be useful to see how other frequency domain techniques compare to the FFT and PSD method during sustained activation of the BRx depressor response. In particular, wavelet transforms and short time Fourier transforms are often utilized in HRV studies, as they have different, but appropriate assumptions for analyzing HRV. Also, it would likely be worthwhile to investigate a frequency modulation model of HRV in this experiment, as the relationship between the baseline and stimulation recordings is highly analogous to frequency modulation.

4.7 Refining the Experimental Protocol

The experimental protocol could be improved to better assess spontaneous animal stability. Based on the findings in this work, there are at least two main additions to the protocol that could greatly assist in assessing cardiovascular stability:

1. Creating a live display of the animal's ECG histogram, whereby a continuously moving ten-minute interval of ECG histogram is visually monitored

2. Creating a live display of the FFT of the BP profile, which could be used to immediately assess respiration rate. This would be particularly useful in determining if the animal is accepting the respirator.

4.8 Conclusion

Overall, it was found that the most meaningful frequency-based measurements of HRV are focused on PNS activity, particularly with measurements focused on the respiratory band. Based on the measurements in this work, there is strong potential in three HRV measures utilizing the FFT and PSD method:

1. Integrating HF band absolute power in gaussian data (more ns needed)
2. Integrating respiratory peak power for $\alpha = 10\%$ in gaussian data
3. Integrating respiratory peak power for $\alpha = 5\%$ in gaussian data

In these measurements, it is crucial to restrict data sets appropriately based on animal stability. Given the high levels of significance measured with respiratory peak analysis, there is sufficient evidence to reject the null hypothesis.

REFERENCES

REFERENCES

[1] "Achievements in public health, 1900-1999: Decline in deaths from heart disease and stroke – united states, 1900-1999." 2001, May 2 1999. [Online]. Available: https://www.cdc.gov/mmwr/preview/mmwrhtml/mm4830a1.htm

[2] "The fcats about high blood pressure." 2017, Nov 30 2020. [Online]. Available: https://www.heart.org/en/health-topics/high-blood-pressure/the-facts-about-high-blood-pressure

[3] "Electrocardiogram (ecg or ekg)." 2020 2020. [Online]. Available: https://www.heart.org/en/health-topics/heart-attack/diagnosing-a-heart-attack/electrocardiogram-ecg-or-ekg

[4] A. H. Association, "How the healthy heart works," 2020. [Online]. Available: https://www.heart.org/en/health-topics/congenital-heart-defects/about-congenital-heart-defects/how-the-healthy-heart-works

[5] I. Tonhajzerova, M. Mestanik, A. Mestanikova, and A. Jurko, "Respiratory sinus arrhythmia as a non-invasive index of 'brain-heart' interaction in stress," *Indian J Med Res*, vol. 144, no. 6, pp. 815–822, 2016. [Online]. Available: https://www.ncbi.nlm.nih.gov/pubmed/28474618

[6] M. Sakakibara, J. Hayano, L. O. Oikawa, M. Katsamanis, and P. Lehrer, "Heart rate variability biofeedback improves cardiorespiratory resting function during sleep," *Appl Psychophysiol Biofeedback*, vol. 38, no. 4, pp. 265–71, 2013. [Online]. Available: https://www.ncbi.nlm.nih.gov/pubmed/23959190

[7] J. P. Moak, D. S. Goldstein, B. A. Eldadah, A. Saleem, C. Holmes, S. Pechnik, and Y. Sharabi, "Supine low-frequency power of heart rate variability reflects baroreflex function, not cardiac sympathetic innervation," *Heart Rhythm*, vol. 4, no. 12, pp. 1523–9, 2007. [Online]. Available: https://www.ncbi.nlm.nih.gov/pubmed/17997358

[8] L. Mintch, "Sustained stimulus paradigms and sexual dimorphism of the aortic baroreflex in rat," Thesis, 2019.

[9] F. H. Netter, "Relation of action potential from the various cardiac region to the body surface ecg," 2020.

[10] J. Betts, P. Desaix, E. Johnson, J. Johnson, O. Korol, D. Kruse, B. Poe, O. College, J. Wise, and M. Womble, *Anatomy Physiology*. OpenStax College, Rice University, 2013. [Online]. Available: https://books.google.com/books?id=dvVgngEACAAJ

[11] A. D. Loewy and K. M. Spyer, *Central regulation of autonomic functions*. New York: Oxford University Press, 1990.

[12] S. Akselrod, D. Gordon, F. A. Ubel, D. C. Shannon, A. C. Berger, and R. J. Cohen, "Power spectrum analysis of heart rate fluctuation: a quantitative probe of beat-to-beat cardiovascular control," *Science*, vol. 213, no. 4504, pp. 220–2, 1981. [Online]. Available: https://www.ncbi.nlm.nih.gov/pubmed/6166045

[13] R. Bartels, L. Neumamm, T. Pecanha, and A. R. S. Carvalho, "Sinuscor: an advanced tool for heart rate variability analysis," *Biomed Eng Online*, vol. 16, no. 1, p. 110, 2017. [Online]. Available: https://www.ncbi.nlm.nih.gov/pubmed/28923061

[14] D. M. Bloomfield, S. Zweibel, J. Bigger, J. T., and R. C. Steinman, "R-r variability detects increases in vagal modulation with phenylephrine infusion," *Am J Physiol*, vol. 274, no. 5, pp. H1761–6, 1998. [Online]. Available: https://www.ncbi.nlm.nih.gov/pubmed/9612388

[15] V. J. Dias da Silva, R. Miranda, L. Oliveira, C. H. Rodrigues Alves, G. H. Van Gils, A. Porta, and N. Montano, "Heart rate and arterial pressure variability and baroreflex sensitivity in ovariectomized spontaneously hypertensive rats," *Life Sci*, vol. 84, no. 21-22, pp. 719–24, 2009. [Online]. Available: https://www.ncbi.nlm.nih.gov/pubmed/19249314

[16] D. Eddie, E. Vaschillo, B. Vaschillo, and P. Lehrer, "Heart rate variability biofeedback: Theoretical basis, delivery, and its potential for the treatment of substance use disorders," *Addict Res Theory*, vol. 23, no. 4, pp. 266–272, 2015. [Online]. Available: https://www.ncbi.nlm.nih.gov/pubmed/28077937

[17] J. J. Goldberger, "Sympathovagal balance: how should we measure it?" *Am J Physiol*, vol. 276, no. 4, pp. H1273–80, 1999. [Online]. Available: https://www.ncbi.nlm.nih.gov/pubmed/10199852

[18] J. J. Goldberger, S. Challapalli, R. Tung, M. A. Parker, and A. H. Kadish, "Relationship of heart rate variability to parasympathetic effect," *Circulation*, vol. 103, no. 15, pp. 1977–83, 2001. [Online]. Available: https://www.ncbi.nlm.nih.gov/pubmed/11306527

[19] M. V. Kamath, M. A. Watanabe, and A. R. M. Upton, *Heart rate variability (HRV) signal analysis : clinical applications*. Boca Raton: CRC Press, 2013.

[20] N. Montano, T. G. Ruscone, A. Porta, F. Lombardi, M. Pagani, and A. Malliani, "Power spectrum analysis of heart rate variability to assess the changes in sympathovagal balance during graded orthostatic tilt," *Circulation*, vol. 90, no. 4, pp. 1826–31, 1994. [Online]. Available: https://www.ncbi.nlm.nih.gov/pubmed/7923668

[21] L. Rodriguez-Linares, M. J. Lado, X. A. Vila, A. J. Mendez, and P. Cuesta, "ghrv: Heart rate variability analysis made easy," *Comput Methods Programs Biomed*, vol. 116, no. 1, pp. 26–38, 2014. [Online]. Available: https://www.ncbi.nlm.nih.gov/pubmed/24854108

[22] L. C. Silveira, G. C. Tezini, D. S. Schujmann, J. M. Porto, B. R. Rossi, and H. C. Souza, "Comparison of the effects of aerobic and

resistance training on cardiac autonomic adaptations in ovariectomized rats," *Auton Neurosci*, vol. 162, no. 1-2, pp. 35–41, 2011. [Online]. Available: https://www.ncbi.nlm.nih.gov/pubmed/21429820

[23] P. Sleight, "The importance of the autonomic nervous system in health and disease," *Aust N Z J Med*, vol. 27, no. 4, pp. 467–73, 1997. [Online]. Available: https://www.ncbi.nlm.nih.gov/pubmed/9448899

[24] A. Voss, R. Schroeder, A. Heitmann, A. Peters, and S. Perz, "Short-term heart rate variability–influence of gender and age in healthy subjects," *PLoS One*, vol. 10, no. 3, p. e0118308, 2015. [Online]. Available: https://www.ncbi.nlm.nih.gov/pubmed/25822720

[25] R. Freeman and M. W. Chapleau, "Testing the autonomic nervous system," *Handb Clin Neurol*, vol. 115, pp. 115–36, 2013. [Online]. Available: https://www.ncbi.nlm.nih.gov/pubmed/23931777

[26] P. M. Lehrer, "Heart rate variability biofeedback and other psychophysiological procedures as important elements in psychotherapy," *Int J Psychophysiol*, vol. 131, pp. 89–95, 2018. [Online]. Available: https://www.ncbi.nlm.nih.gov/pubmed/28935225

[27] P. M. Lehrer and R. Gevirtz, "Heart rate variability biofeedback: how and why does it work?" *Front Psychol*, vol. 5, p. 756, 2014. [Online]. Available: https://www.ncbi.nlm.nih.gov/pubmed/25101026

[28] H. Nishimura and M. Yamasaki, "Changes in blood pressure, blood flow towards the head and heart rate during 90 deg head-up tilting for 30 min in anaesthetized male rats," *Exp Physiol*, vol. 103, no. 1, pp. 31–39, 2018. [Online]. Available: https://www.ncbi.nlm.nih.gov/pubmed/29086448

[29] G. C. Tezini, L. C. Silveira, J. Villa-Cle, P. G., C. P. Jacinto, T. H. Di Sacco, and H. C. Souza, "The effect of aerobic physical training on cardiac autonomic control of rats submitted to ovariectomy," *Menopause*, vol. 16, no. 1, pp. 110–6, 2009. [Online]. Available: https://www.ncbi.nlm.nih.gov/pubmed/18978639

[30] D. S. Goldstein, O. Bentho, M. Y. Park, and Y. Sharabi, "Low-frequency power of heart rate variability is not a measure of cardiac sympathetic tone but may be a measure of modulation of cardiac autonomic outflows by baroreflexes," *Exp Physiol*, vol. 96, no. 12, pp. 1255–61, 2011. [Online]. Available: https://www.ncbi.nlm.nih.gov/pubmed/21890520

[31] M. W. Ahmed, A. H. Kadish, M. A. Parker, and J. J. Goldberger, "Effect of physiologic and pharmacologic adrenergic stimulation on heart rate variability," *J Am Coll Cardiol*, vol. 24, no. 4, pp. 1082–90, 1994. [Online]. Available: https://www.ncbi.nlm.nih.gov/pubmed/7930202

[32] L. Bernardi, J. Wdowczyk-Szulc, C. Valenti, S. Castoldi, C. Passino, G. Spadacini, and P. Sleight, "Effects of controlled breathing, mental activity and mental stress with or without verbalization on heart rate variability," *J Am Coll Cardiol*, vol. 35, no. 6, pp. 1462–9, 2000. [Online]. Available: https://www.ncbi.nlm.nih.gov/pubmed/10807448

[33] J. Hayano and E. Yuda, "Pitfalls of assessment of autonomic function by heart rate variability," *J Physiol Anthropol*, vol. 38, no. 1, p. 3, 2019.

[34] H. B. Hopf, A. Skyschally, G. Heusch, and J. Peters, "Low-frequency spectral power of heart rate variability is not a specific marker of cardiac sympathetic modulation," *Anesthesiology*, vol. 82, no. 3, pp. 609–19, 1995. [Online]. Available: https://www.ncbi.nlm.nih.gov/pubmed/7879929

[35] N. Igosheva, O. Klimova, T. Anishchenko, and V. Glover, "Prenatal stress alters cardiovascular responses in adult rats," *J Physiol*, vol. 557, no. Pt 1, pp. 273–85, 2004. [Online]. Available: https://www.ncbi.nlm.nih.gov/pubmed/15034122

[36] C. Kruger, A. Kalenka, A. Haunstetter, M. Schweizer, C. Maier, U. Ruhle, H. Ehmke, W. Kubler, and M. Haass, "Baroreflex sensitivity and heart rate variability in conscious rats with myocardial infarction," *Am J Physiol*, vol. 273, no. 5, pp. H2240–7, 1997. [Online]. Available: https://www.ncbi.nlm.nih.gov/pubmed/9374759

[37] M. Kuwahara, K. Yayou, K. Ishii, S. Hashimoto, H. Tsubone, and S. Sugano, "Power spectral analysis of heart rate variability as a new method for assessing autonomic activity in the rat," *J Electrocardiol*, vol. 27, no. 4, pp. 333–7, 1994. [Online]. Available: https://www.ncbi.nlm.nih.gov/pubmed/7815012

[38] M. Pagani, R. Sala, M. Malacarne, and D. Lucini, "Benchmarking heart rate variability to overcome sex-related bias," *Adv Exp Med Biol*, vol. 1065, pp. 191–205, 2018. [Online]. Available: https://www.ncbi.nlm.nih.gov/pubmed/30051386

[39] J. K. Phillips, "Autonomic dysfunction in heart failure and renal disease," *Front Physiol*, vol. 3, p. 219, 2012. [Online]. Available: https://www.ncbi.nlm.nih.gov/pubmed/22740834

[40] G. D. Spina, B. B. Gonze, A. C. B. Barbosa, E. F. Sperandio, and V. Z. Dourado, "Presence of age- and sex-related differences in heart rate variability despite the maintenance of a suitable level of accelerometer-based physical activity," *Braz J Med Biol Res*, vol. 52, no. 8, p. e8088, 2019. [Online]. Available: https://www.ncbi.nlm.nih.gov/pubmed/31389489

[41] J. Koenig and J. F. Thayer, "Sex differences in healthy human heart rate variability: A meta-analysis," *Neurosci Biobehav Rev*, vol. 64, pp. 288–310, 2016. [Online]. Available: https://www.ncbi.nlm.nih.gov/pubmed/26964804

[42] M. Hansson-Sandsten and P. Jonsson, "Multiple window correlation analysis of hrv power and respiratory frequency," *IEEE Trans Biomed Eng*, vol. 54, no. 10, pp. 1770–9, 2007. [Online]. Available: https://www.ncbi.nlm.nih.gov/pubmed/17926675

[43] J. S. Gasior, J. Sacha, P. J. Jelen, M. Pawlowski, B. Werner, and M. J. Dabrowski, "Interaction between heart rate variability and heart rate in pediatric population," *Front Physiol*, vol. 6, p. 385, 2015. [Online]. Available: https://www.ncbi.nlm.nih.gov/pubmed/26733878

[44] C. Campos, K. R. Casali, D. Baraldi, A. Conzatti, A. S. Araujo, N. Khaper, S. Llesuy, K. Rigatto, and A. Bello-Klein, "Efficacy of a low dose of estrogen on antioxidant defenses and heart rate variability," *Oxid Med Cell Longev*, vol. 2014, p. 218749, 2014. [Online]. Available: https://www.ncbi.nlm.nih.gov/pubmed/24738017

[45] C. Cerutti, C. Barres, and C. Paultre, "Baroreflex modulation of blood pressure and heart rate variabilities in rats: assessment by spectral analysis," *Am J Physiol*, vol. 266, no. 5 Pt 2, pp. H1993–2000, 1994. [Online]. Available: https://www.ncbi.nlm.nih.gov/pubmed/8203598

[46] P. J. Gengo, N. Bowling, V. L. Wyss, and J. S. Hayes, "Effects of prolonged phenylephrine infusion on cardiac adrenoceptors and calcium channels," *J Pharmacol Exp Ther*, vol. 244, no. 1, pp. 100–5, 1988. [Online]. Available: https://www.ncbi.nlm.nih.gov/pubmed/2447272

[47] J. J. Goldberger, M. W. Ahmed, M. A. Parker, and A. H. Kadish, "Dissociation of heart rate variability from parasympathetic tone," *Am J Physiol*, vol. 266, no. 5 Pt 2, pp. H2152–7, 1994. [Online]. Available: https://www.ncbi.nlm.nih.gov/pubmed/8203614

[48] J. J. Goldberger, Y. H. Kim, M. W. Ahmed, and A. H. Kadish, "Effect of graded increases in parasympathetic tone on heart rate variability," *J Cardiovasc Electrophysiol*, vol. 7, no. 7, pp. 594–602, 1996. [Online]. Available: https://www.ncbi.nlm.nih.gov/pubmed/8807405

[49] G. B. Guo and F. M. Abboud, "Angiotensin ii attenuates baroreflex control of heart rate and sympathetic activity," *Am J Physiol*, vol. 246, no. 1 Pt 2, pp. H80–9, 1984. [Online]. Available: https://www.ncbi.nlm.nih.gov/pubmed/6696093

[50] S. N. Iyer and M. J. Katovich, "Vascular reactivity to phenylephrine and angiotensin ii in hypertensive rats associated with insulin resistance," *Clin Exp Hypertens*, vol. 18, no. 2, pp. 227–42, 1996. [Online]. Available: https://www.ncbi.nlm.nih.gov/pubmed/8869002

[51] Y. H. Kim, M. W. Ahmed, A. H. Kadish, and J. J. Goldberger, "Characterization of the factors that determine the effect of sympathetic stimulation on heart rate variability," *Pacing Clin Electrophysiol*, vol. 20, no. 8 Pt 1, pp. 1936–46, 1997. [Online]. Available: https://www.ncbi.nlm.nih.gov/pubmed/9272531

[52] J. A. Moffitt, A. J. Grippo, and A. K. Johnson, "Baroreceptor reflex control of heart rate in rats studied by induced and autogenic changes in arterial pressure," *Am J Physiol Heart Circ Physiol*, vol. 288, no. 5, pp. H2422–30, 2005. [Online]. Available: https://www.ncbi.nlm.nih.gov/pubmed/15637128

[53] H. S. Smyth, P. Sleight, and G. W. Pickering, "Reflex regulation of arterial pressure during sleep in man. a quantitative method of assessing baroreflex sensitivity," *Circ Res*, vol. 24, no. 1, pp. 109–21, 1969. [Online]. Available: https://www.ncbi.nlm.nih.gov/pubmed/4303309

[54] G. F. Dibona, "Sympathetic nervous system and hypertension," *Hypertension*, vol. 61, no. 3, pp. 556–560, 2013. [Online]. Available: https://dx.doi.org/10.1161/HYPERTENSIONAHA.111.00633

[55] M. T. La Rovere, G. Specchia, A. Mortara, and P. J. Schwartz, "Baroreflex sensitivity, clinical correlates, and cardiovascular mortality among patients with a first myocardial infarction. a prospective study," *Circulation*, vol. 78, no. 4, pp. 816–24, 1988. [Online]. Available: https://www.ncbi.nlm.nih.gov/pubmed/3168190

[56] S. D. Stocker, A. F. Sved, and M. C. Andresen, "Missing pieces of the piezo1/piezo2 baroreceptor hypothesis: an autonomic perspective," *J Neurophysiol*, vol. 122, no. 3, pp. 1207–1212, 2019. [Online]. Available: https://www.ncbi.nlm.nih.gov/pubmed/31314636

[57] C. A. Swenne, "Baroreflex sensitivity: mechanisms and measurement," *Neth Heart J*, vol. 21, no. 2, pp. 58–60, 2013. [Online]. Available: https://www.ncbi.nlm.nih.gov/pubmed/23179611

[58] M. Henze, D. Hart, A. Samarel, J. Barakat, L. Eckert, and K. Scrogin, "Persistent alterations in heart rate variability, baroreflex sensitivity, and anxiety-like behaviors during development of heart failure in the rat," *Am J Physiol Heart Circ Physiol*, vol. 295, no. 1, pp. H29–38, 2008. [Online]. Available: https://www.ncbi.nlm.nih.gov/pubmed/18456727

[59] "Heart rate variability: standards of measurement, physiological interpretation and clinical use. task force of the european society of cardiology and the north american society of pacing and electrophysiology," *Circulation*, vol. 93, no. 5, pp. 1043–65, 1996. [Online]. Available: https://www.ncbi.nlm.nih.gov/pubmed/8598068

[60] T. Cui, "Spectrum analysis of heart rate variability," Master's Degree, 2013.

[61] R. A. Harrigan, A. D. Perron, and W. J. Brady, "Atrioventricular dissociation," *Am J Emerg Med*, vol. 19, no. 3, pp. 218–22, 2001. [Online]. Available: https://www.ncbi.nlm.nih.gov/pubmed/11326350

[62] L. E. V. Silva, V. R. Geraldini, B. P. de Oliveira, C. A. A. Silva, A. Porta, and R. Fazan, "Comparison between spectral analysis and symbolic dynamics for heart rate variability analysis in the rat," *Sci Rep*, vol. 7, no. 1, p. 8428, 2017. [Online]. Available: https://www.ncbi.nlm.nih.gov/pubmed/28814785

[63] T. B. Kuo, C. J. Lai, Y. T. Huang, and C. C. Yang, "Regression analysis between heart rate variability and baroreflex-related vagus nerve activity in rats," *J Cardiovasc Electrophysiol*, vol. 16, no. 8, pp. 864–9, 2005. [Online]. Available: https://www.ncbi.nlm.nih.gov/pubmed/16101628

[64] J. Fazan, R., M. de Oliveira, V. J. da Silva, L. F. Joaquim, N. Montano, A. Porta, M. W. Chapleau, and H. C. Salgado, "Frequency-dependent baroreflex modulation of blood pressure and heart rate variability in conscious mice," *Am J Physiol Heart Circ Physiol*, vol. 289, no. 5, pp. H1968–75, 2005. [Online]. Available: https://www.ncbi.nlm.nih.gov/pubmed/15951338